Pulse shaping and compression by second-harmonic generation with quasi-phase-matching gratings in the presence of arbitrary dispersion

G. Imeshev, M. A. Arbore,* S. Kasriel,† and M. M. Fejer

E. L. Ginzton Laboratory, Stanford University, Stanford, California 94305

Received January 3, 2000; revised manuscript received April 18, 2000

A theoretical treatment of group-velocity dispersion and higher-order dispersion effects on the second-harmonic-generation (SHG) process with longitudinally nonuniform quasi-phase-matching (QPM) gratings is presented. We show how these dispersion terms can be accounted for in the design of a QPM-SHG pulse shaper. Our numerical simulation results show that, if the proper dispersion correction is included in the QPM grating design, one can generate sub-10-fs transform-limited pulses at 400 nm by doubling the output of a Ti:sapphire oscillator. © 2000 Optical Society of America [S0740-3224(00)00808-0]

OCIS codes: 140.7090, 190.7110, 190.2620, 190.4360, 230.4320, 320.5520, 320.5540, 320.7110, 320.7080.

1. INTRODUCTION

Frequency doubling of ultrashort pulses is a powerful and versatile technique for converting laser pulses to wavelength regions in which direct generation is difficult or even impossible. For such ultrafast frequency converters, the dispersive properties of the nonlinear optical material play a crucial role. In general, pulses at different wavelengths propagate through a medium with different group velocities, leading to temporal walk-off. This group-velocity mismatch (GVM) between the first-harmonic (FH) and the second-harmonic (SH) pulses puts a restriction on the length of the nonlinear crystal that can be used to generate the SH pulses without substantial broadening relative to the FH pulses.[1–5] This characteristic length is called a group-velocity walk-off length, L_{gv}, and is defined as $L_{gv} = \tau_0/|\delta v|$, where τ_0 is the initial pulse length of the transform-limited FH pulse and the GVM parameter $\delta v = 1/u_1 - 1/u_2$, with u_1 and u_2 being the FH and the SH group velocities, respectively.

Intrapulse group-velocity dispersion (GVD), a second-order effect in comparison with GVM, is generally not significant in single-pass devices shorter than one walk-off length and hence can be neglected, provided that this condition is satisfied. When a short pulse propagates through a medium over a length for which GVD is nonnegligible the medium adds some linear chirp to the pulse, proportional to the length traveled, resulting in a change of the shape and amplitude of the pulse.[4,6] The characteristic length over which the GVD effect becomes important is $L_\beta = \tau_0^2/|\beta|$, where β is the GVD coefficient. Higher-order dispersion beyond GVD leads to even further distortion of the pulse and causes asymmetry in the pulse profile.[4,6] For a given length of the nonlinear medium, GVD and higher-order dispersion become increasingly important for shorter pulses and/or toward shorter wavelengths, in the case of normal dispersion. The effects of GVD during second-harmonic generation (SHG) in uniform crystals, in particular, the dispersive shaping of the pulses caused by GVD, were previously considered in the literature.[7,8]

Recently, microstructured quasi-phase-matching (QPM) materials have been used in ultrafast frequency conversion devices. QPM[9,10] offers the benefits of using noncritical propagation geometries and large nonlinear coefficients. More importantly, for ultrafast applications, QPM provides extra degrees of freedom in engineering the amplitude and phase responses of the frequency converter, a function not available with conventional birefringent phase matching. QPM devices have been used to combine such ultrafast techniques as pulse shaping and compression with frequency conversion in compact and monolithic devices.[11–17] These devices require that the length of the QPM grating be at least several walk-off lengths long,[18,19] and hence GVD will have a noticeable effect that must be taken into account.

We have already presented a theoretical treatment of the SHG process with longitudinally nonuniform QPM gratings in the undepleted pump approximation in Ref. 19. In that work we used a frequency-domain analysis to obtain an expression for the generated SH field in an integral form, valid for arbitrary material dispersion and an arbitrarily modulated QPM grating. Neglecting GVD and higher-order dispersion, we arrived at a simpler expression for the SH field, which had the form of a transfer function in the frequency domain. Even though this transfer function formalism is restricted to cases in which dispersion beyond GVM is negligible, it allowed us to de-

0740-3224/2000/081420-18$15.00

rive the essential features of pulse shaping and compression, which rely on the GVM and the spatial localization of conversion in a longitudinally nonuniform grating. The advantage of such a transfer function relation is that it enabled us to obtain a straightforward explicit procedure for the design of the grating function required for a particular shaping function. We analyzed in detail a particular case of shaping: pulse compression with linearly chirped gratings.

The theoretical treatment in this paper is based on results obtained in Ref. 19. Here we present a detailed treatment of the GVD and higher-order material dispersion effects and show how they can be accounted for in the design of a QPM-SHG pulse shaper. This paper is organized as follows. In Section 2 we give an intuitive time-domain description of the process and indicate how these time-domain considerations can be used to design a chirped grating compressor for cases in which GVD and higher-order dispersion are nonnegligible. In Section 3 we introduce the mathematical formalism for description of longitudinally nonuniform QPM gratings by representing the modulated nonlinear coefficient as a sum of its spatial Fourier components with slowly varying amplitudes. In Section 4 we present a general expression for the SH field generated in a nonuniform QPM grating, valid for arbitrary dispersion, as well as the transfer function result in the limiting case of negligible GVD and higher-order dispersion, as originally derived in Ref. 19. We also find that a similar transfer function relation exists for arbitrary dispersion at the SH as long as GVD and higher-order dispersion at the FH are negligible. In Section 5 we consider the effects of GVD on the cw SHG tuning curves with uniform QPM gratings. In Section 6 we consider the performance of a linearly chirped grating as a compressor in the case of nonnegligible GVD at the SH and show that, to first order, a linearly chirped grating will still compensate for the quadratic phase of the FH pulse, whereas the optimum grating chirp for compression is shifted from that in the negligible-GVD case. In Section 7, by assuming that in a strongly chirped grating conversion of each spectral component occurs over a distance that is small as compared with the grating length, we develop a procedure for choosing the necessary grating function for arbitrary pulse shaping in the presence of arbitrary dispersion. Section 8 presents the analytical treatment of the selection of the appropriate grating function for compression. While the treatment in this section is limited to linearly chirped Gaussian pulses and no dispersion beyond GVD, it does not require the assumption of localized conversion, which is used in Section 7. In Section 9 we present the results of numerical modeling of pulse compression with several different pulse shapes: Gaussian, hyperbolic secant, and sinclike (as characteristic for pulses with top-hat spectra). We predict that, if the dispersion is accounted for according to design rules developed in Sections 7 and 8, generation of transform-limited sub-10-fs pulses at 400 nm is possible by doubling of stretched pulses at 800 nm with a pulse length of 10 fs before stretching. Section 10 presents the comparison of the dispersion data for several common QPM ferroelectrics. Finally, we summarize the results of this paper in Section 11.

2. TIME-DOMAIN PICTURE OF PULSE SHAPING AND COMPRESSION WITH NONUNIFORM QUASI-PHASE-MATCHING GRATINGS IN THE PRESENCE OF GROUP-VELOCITY DISPERSION

Pulse compression with longitudinally nonuniform QPM gratings, a particular case of more-general pulse shaping, can be most intuitively understood in the time domain. It relies on the combination of two phenomena: the dispersion of group velocities, which is a material property, and spatial localization of the SHG process, determined by the local k-vector of the QPM grating, which can be engineered. To first order, dispersion causes FH and SH pulses to propagate with different group velocities, u_1 and u_2, respectively, leading to the GVM. If the second-order dispersion (GVD) and higher-order dispersion are negligible, all frequency components within the spectrum of a particular pulse will propagate with the same group velocity. More importantly, all frequency components of the nonlinear polarization wave, which drives the conversion and is proportional to the square of the FH pulse temporal profile, propagate with the same group velocity u_1 as the components of the FH pulse itself. A particular frequency component of the nonlinear polarization generates the SH component at the same frequency at some location z_0 in the crystal, where the grating local k-vector is equal to the k-vector mismatch evaluated for this frequency (i.e., meets the phase-matching condition). It takes a certain time (the group delay time), determined by u_1 and the initial chirp of the FH pulse, for this component to arrive at position z_0. After the SH field is generated it travels toward the exit of the crystal with group velocity $u_2 \neq u_1$. The grating design procedure for pulse compression is then to require that the conversion locations for different spectral components be selected such that these SH frequency components arrive at the output of the grating at the same time, thus requiring a linearly chirped grating if it is to generate a compressed SH pulse.

If the second-order dispersion (GVD) and the higher-order dispersion are nonnegligible, different spectral components within each pulse will propagate with different group velocities. Moreover, the propagation law for the frequency components of the nonlinear polarization is different from that of the FH pulse, resulting in a more complicated accounting of the group delay for different components. The time-domain cartoon approach described above for the negligible-GVD case still allows derivation of the grating chirp required for compression in the presence of GVD and produces a result that is almost the same as that of the more accurate frequency-domain analysis, presented in Sections 7 and 8. The grating chirp, required for compression in the presence of GVD, is not linear with distance.

This simplified time-domain description assumes that the conversion process for each frequency component is localized at a point. Even though this assumption is not rigorously correct, the advantage of the approximate approach is that it is applicable to more-general cases than can be handled with the exact method of Section 8. This localization of conversion assumption is put into more

mathematically rigorous terms by the stationary phase method described in Section 7.

We also note that, to achieve a uniform conversion for all components when GVD is present, the grating amplitude should be modulated along z; otherwise, different components will be converted with different efficiencies. This is a result of two effects. First, the GVD results not only in the position-dependent spreading of frequency components but also in a change of the amplitude of the nonlinear polarization along the propagation direction, which must be compensated for by the amplitude of the QPM grating. We can understand the second effect causing the efficiency nonuniformity for different components by realizing that the conversion is not happening at a point where the phase-matching condition is satisfied exactly but rather that it occurs over a finite range of grating k-vectors. As the rate at which the grating k-vector changes with distance is not constant for nonlinearly chirped gratings, the distance over which a particular frequency component is phase matched also varies, leading to different efficiencies for different frequency components.

3. LONGITUDINALLY NONUNIFORM QUASI-PHASE-MATCHING GRATINGS

QPM gratings generally use sign reversal of the nonlinear coefficient along the crystal length in a periodic or aperiodic fashion; i.e., mathematically, $d(z)$ is a square wave whose amplitude is the intrinsic nonlinear coefficient of the material, d_{eff}. Assuming that period and duty cycle modulations are slow, $d(z)$ can be decomposed into the spatial Fourier components $d_m(z)$ with slowly varying amplitudes and phases:

$$d(z) = \sum_{m=-\infty}^{\infty} d_m(z) = \sum_{m=-\infty}^{\infty} |d_m(z)| \exp[iK_{0m}z + i\varphi_m(z)], \quad (3.1)$$

where we explicitly factored out the linear component, $K_{0m}z$, of the total phase of each Fourier component of the grating, $\Phi_m(z) \equiv K_{0m}z + \varphi_m(z)$. The carrier k-vector of the grating is $K_{0m} = 2\pi m/\Lambda_0$, where Λ_0 is the nominal period for QPM. The local k-vector of the grating is then

$$K_m(z) = \frac{d\Phi_m}{dz} = K_{0m} + \frac{d\varphi_m}{dz} \quad (3.2)$$

and is related to the local QPM period $\Lambda(z)$ as $K_m(z) = 2\pi m/\Lambda(z)$. Since $\Lambda(z)$ is engineerable, the position-dependent k-vector of an appropriate Fourier component of the grating is engineerable too.

In Eq. (3.1), $|d_m(z)|$ is the amplitude of the mth Fourier component of the grating, which is related to the local grating duty cycle $G(z)$ as[10]

$$|d_m(z)| = \frac{2}{\pi m} d_{\text{eff}} \sin[\pi m G(z)], \quad (3.3)$$

and hence can also be engineered by control of the local duty cycle of the square grating. If $G(z) = 0$, i.e., the material is unmodulated, then $|d_m(z)| = 0$, which indicates that there is no modulated component of the QPM grating. The maximum value of $|d_m(z)|$ is $(2/\pi m)d_{\text{eff}}$, which is achieved at $G = 0.5$ for an odd order or at $G = 1/(2m)$ for an even-order QPM process.

For the analysis presented in this paper we assume that different Fourier components of the QPM grating do not overlap in k space and that spectra of the interacting pulses are narrow enough such that they interact with only one QPM order. Consequently, the modulated nonlinear coefficient $d(z)$ will be represented by only one relevant Fourier component, and from now on we will omit its QPM order subscript m. We note, however, that the ability to utilize different QPM orders of the same grating can be advantageous for phase matching several nonlinear processes simultaneously.[20–25]

4. GENERAL DESCRIPTION OF THE SECOND-HARMONIC-GENERATION PROCESS IN THE FREQUENCY DOMAIN

We start the analysis by considering a QPM grating of length L with longitudinally modulated nonlinear coefficient $d(z)$. We describe the interacting FH and SH fields with the frequency-domain electric field envelopes, as introduced and discussed in detail in Ref. 19. These envelopes have the frequency-dependent k-vector $k(\omega)$ explicitly factored out and are defined by

$$\hat{E}(z, \omega) = \hat{A}(z, \Omega)\exp[-ik(\omega_0 + \Omega)z], \quad (4.1)$$

where $\hat{E}(z, \omega)$ is the Fourier transform of the electric field, $\hat{A}(z, \Omega)$ is the frequency-domain envelope, and $\Omega = \omega - \omega_0$ is the frequency detuning from the optical carrier frequency ω_0. These envelopes are to be distinguished from the conventional time-domain envelopes $B(z, t)$, which are defined by

$$E(z, t) = B(z, t)\exp(i\omega_0 t - ik_0 z), \quad (4.2)$$

where $E(z,t)$ is the electric field and $k_0 \equiv k(\omega_0)$ is the carrier k-vector.

Assuming the validity of the slowly varying amplitude approximation, an undepleted pump, and a plane-wave interaction, the coupled wave equations governing the propagation of the FH envelope $\hat{A}_1(z, \Omega)$ and the SH envelope $\hat{A}_2(z, \Omega)$ were obtained in Ref. 19 as follows (here and in the remainder of the paper we use the subscript 1 to denote the FH and the subscript 2 to denote the SH):

$$\frac{\partial}{\partial z}\hat{A}_1(z, \Omega) = 0, \quad (4.3)$$

$$\frac{\partial}{\partial z}\hat{A}_2(z, \Omega) = -i\frac{\mu_0\omega_2^2}{2k_2}\hat{P}_{\text{NL}}(z, \Omega)\exp[ik(\omega_2 + \Omega)z], \quad (4.4)$$

where $\Omega = \omega - \omega_2$ is the detuning from the carrier frequency of the SH pulse. In Eq. (4.4) the nonlinear polarization $\hat{P}_{\text{NL}}(z, \Omega)$ is

$$\hat{P}_{\mathrm{NL}}(z,\Omega) = \varepsilon_0 d(z)\int_{-\infty}^{+\infty}\hat{A}_1(z,\Omega')\hat{A}_1(z,\Omega-\Omega') \times \exp\{-i[k(\omega_1+\Omega') + k(\omega_1+\Omega-\Omega')]z\}\mathrm{d}\Omega'. \quad (4.5)$$

Equation (4.3) describes free propagation of the FH wave through the dispersive medium; its solution is

$$\hat{A}_1(z,\Omega) = \hat{A}_1(\Omega), \quad (4.6)$$

where $\hat{A}_1(\Omega) \equiv \hat{A}_1(z=0,\Omega)$ is the envelope at the input ($z=0$) of the grating. The FH frequency-domain envelope is independent of z, even though the pulse does experience dispersive broadening, as can be obtained from Eq. (4.6) through Eq. (4.1) as

$$\hat{E}_1(z,\omega) = \hat{E}_1(z=0,\omega)\exp[-ik(\omega)z], \quad (4.7)$$

which is a result well known from the literature.[4,6]

Substituting the solution for the FH envelope, Eq. (4.6), into the expression for $\hat{P}_{\mathrm{NL}}(z,\Omega)$, Eq. (4.5), and integrating Eq. (4.4) with this result for $\hat{P}_{\mathrm{NL}}(z,\Omega)$, we obtain the output envelope of the SH pulse, $\hat{A}_2(L,\Omega)$, as

$$\hat{A}_2(L,\Omega) = \int_{-\infty}^{+\infty}\hat{A}_1(\Omega')\hat{A}_1(\Omega-\Omega')\hat{d}[\Delta k(\Omega,\Omega')]\mathrm{d}\Omega'. \quad (4.8)$$

The $\hat{d}[\Delta k(\Omega,\Omega')]$ factor in Eq. (4.8) is proportional to the spatial Fourier transform of $d(z)$, with $\Delta k(\Omega,\Omega')$ serving as the transform variable:

$$\hat{d}(\Delta k) = -i\gamma\int_{-\infty}^{+\infty} d(z)\exp(-i\Delta k z)\mathrm{d}z, \quad (4.9)$$

where $\gamma \equiv 2\pi/\lambda_1 n_2$, λ_1 is the free-space FH wavelength, and n_2 is the refractive index at the SH frequency. We extended the limits of integration in Eq. (4.9) from $[0, L]$ to $(-\infty, +\infty)$ by defining $d(z) \equiv 0$ outside the grating. The k-vector mismatch $\Delta k(\Omega,\Omega')$ is defined as

$$\Delta k(\Omega,\Omega') = k(\omega_1+\Omega') + k(\omega_1+\Omega-\Omega') - k(\omega_2+\Omega). \quad (4.10)$$

Performing the Taylor expansion of Eq. (4.10), we obtain $\Delta k(\Omega,\Omega')$ as a sum of Ω'-independent and Ω'-dependent terms,

$$\Delta k(\Omega,\Omega') = \Delta k'(\Omega) + \Delta k''(\Omega,\Omega'), \quad (4.11)$$

with

$$\Delta k'(\Omega) \equiv \Delta k_0 + \delta\nu\Omega + \tfrac{1}{2}\delta\beta\Omega^2 + \delta k'(\Omega), \quad (4.12)$$

$$\Delta k''(\Omega,\Omega') \equiv \beta_1(\Omega'^2 - \Omega\Omega') + \delta k''(\Omega,\Omega'), \quad (4.13)$$

where $\Delta k_0 = 2k_1 - k_2$ is the carrier k-vector mismatch, $\delta\nu = 1/u_1 - 1/u_2$ is the GVM parameter with the group velocities $u_i = [\mathrm{d}k(\omega)/\mathrm{d}\omega]^{-1}|_{\omega=\omega_i}$, and $\delta\beta = \beta_1 - \beta_2$ is the GVD mismatch parameter with the GVD parameters $\beta_i = [\mathrm{d}^2k(\omega)/\mathrm{d}\omega^2]|_{\omega=\omega_i}$. The remainder term $\delta k'(\Omega)$ is of the order of Ω^3, and the remainder term $\delta k''(\Omega,\Omega')$ is of the order of Ω^3 and Ω'^3; in principle, these terms can be written out for arbitrarily high dispersion order. Note that in the ultrafast literature it is common to use β_2 for the GVD coefficient of the dispersive material at a particular wavelength. Here, however, for notational simplicity we use β_i for the GVD coefficient, with the subscript referring to either the FH or the SH.

Equations (4.8)–(4.10) are fairly general results, valid for arbitrary pulse shapes, pulse durations, and dispersion, as long as the undepleted pump and slowly varying amplitude approximations are valid assumptions. Equation (4.8) is an explicit expression for finding the output SH envelope $\hat{A}_2(L,\Omega)$, given (i) the input FH envelope $\hat{A}_1(\Omega)$, (ii) the dispersion properties of the medium, represented by $\Delta k(\Omega,\Omega')$, and (iii) the spatially modulated nonlinear coefficient $d(z)$. However, from a practical standpoint, since the QPM grating function is engineerable, it is desirable to know what grating should be chosen to generate a particular SH pulse, given the available FH pulse, and if implementation of such a design is feasible. In its present form Eq. (4.8) does not provide a ready way to obtain such a design.

In Ref. 19 it was shown that, if GVD and higher-order dispersion terms are negligible, $\hat{d}[\Delta k(\Omega,\Omega')]$ becomes independent of Ω', as is apparent from Eqs. (4.11)–(4.13), and hence can be factored out from under the integral in Eq. (4.8). We introduce new notation for this special case, $\hat{D}_0(\Omega) \equiv \hat{d}(\Delta k_0 + \delta\nu\Omega)$, or, explicitly

$$\hat{D}_0(\Omega) = -i\gamma\int_{-\infty}^{+\infty} d(z)\exp[-i(\Delta k_0 + \delta\nu\Omega)z]\mathrm{d}z. \quad (4.14)$$

From Eq. (4.8) we obtain

$$\hat{A}_2(L,\Omega) = \hat{D}_0(\Omega)\widehat{A_1^2}(\Omega), \quad (4.15)$$

where $\widehat{A_1^2}(\Omega)$ is a self-convolution of $\hat{A}_1(\Omega)$:

$$\widehat{A_1^2}(\Omega) = \int_{-\infty}^{+\infty}\hat{A}_1(\Omega')\hat{A}_1(\Omega-\Omega')\mathrm{d}\Omega'. \quad (4.16)$$

Equation (4.15) is the key result of Ref. 19; it relates the spectra of the FH and the SH through the transfer function $\hat{D}_0(\Omega)$, which depends on the dispersive properties of the medium and on the modulated nonlinear coefficient but not on any of the input or output pulse parameters, and hence can be viewed as a filter in the frequency domain. The advantage of such a transfer function relation, as compared with the more general Eq. (4.8), is that is provides a simple way to design the QPM grating necessary for generation of a desired SH pulse from a given FH pulse. The necessary $\hat{D}_0(\Omega)$ is simply $\hat{A}_2(L,\Omega)/\widehat{A_1^2}(\Omega)$, from which $d(z)$ is obtained with the inverse Fourier transform. We note that Eq. (4.15) is valid for arbitrary pulse shapes and hence is a basis for general pulse shaping with QPM gratings, as long as GVD is negligible.[12,19]

Mathematically, the transfer function result of Eq. (4.15) arises because $\Delta k(\Omega,\Omega')$, as defined by Eqs. (4.11)–(4.13), and hence $\hat{d}(\Delta k)$, are independent of Ω'. We note that the Ω'-dependent part of $\Delta k(\Omega,\Omega')$, $\delta k''(\Omega,\Omega')$, defined by Eq. (4.13), contains only the FH dispersion parameters; all the SH dispersion is accounted for in Eq. (4.12). Hence keeping the GVD and higher-order dispersion terms at the SH [Eq. (4.12)] but neglecting those at the FH still produces a transfer function

result. For this case, we introduce notation for the transfer function, $\hat{D}_2(\Omega) \equiv \hat{d}[\Delta k'(\Omega)]$, or, explicitly,

$$\hat{D}_2(\Omega) = -i\gamma \int_{-\infty}^{+\infty} d(z)\exp[-i\Delta k'(\Omega)z]\mathrm{d}z, \quad (4.17)$$

and the transfer function relation is now

$$\hat{A}_2(L, \Omega) = \hat{D}_2(\Omega)\widehat{A_1^2}(\Omega). \quad (4.18)$$

The transfer function $\hat{D}_2(\Omega)$, as defined by Eq. (4.17), is a generalization of $\hat{D}_0(\Omega)$ and can be used for the design of a general QPM pulse shaping device, in a way similar to the design prescription presented in Ref. 19.

If the GVD at the FH cannot be neglected, the simple transfer function relation does not hold, and one has to use Eq. (4.8). In Section 7 we develop a procedure for the design of the phase of the QPM grating, valid for arbitrary dispersion and pulse shapes, but have to assume a strongly chirped grating for this derivation. In Section 8 we find that, for a restricted class of Gaussian FH pulses with possible linear chirp and no dispersion beyond GVD at the FH, Eq. (4.8) can be integrated in a closed form to yield a relation similar to the transfer function relation of Eqs. (4.15) and (4.18), though with a filter function dependent on the parameters of the input pulse.

5. UNIFORM GRATINGS AND CONTINUOUS-WAVE TUNING CURVES

Let us first consider the effects of GVD on the cw SHG process with a uniform QPM grating. The input FH field is a monochromatic wave with frequency $\omega_1 + \Omega_1$, where Ω_1 is the detuning from the nominal (in the sense of the envelope carrier) FH optical frequency, ω_1. Thus

$$E_1(z = 0, t) = E_1 \exp[i(\omega_1 + \Omega_1)t]. \quad (5.1)$$

The frequency-domain envelope is obtained from Eq. (4.1) as

$$\hat{A}_1(\Omega) = E_1\delta(\Omega - \Omega_1). \quad (5.2)$$

The modulated nonlinear coefficient for the constant-duty-cycle uniform QPM grating of length L and period Λ_0 (and hence with grating k-vector $K_0 = 2\pi/\Lambda_0$) is represented as

$$d(z) = |d|\exp(iK_0 z)\mathrm{rect}\left(\frac{z}{L} - \frac{1}{2}\right), \quad (5.3)$$

where $\mathrm{rect}(x) = 1$ for $|x| \leq 1/2$ and $\mathrm{rect}(x) = 0$ otherwise. Substituting Eqs. (5.2) and (5.3) into Eqs. (4.8)–(4.10), we obtain

$$\hat{A}_2(L, \Omega = 2\Omega_1) = E_1^2\hat{d}[\Delta k(\Omega)], \quad (5.4)$$

where, neglecting a phase factor linear in Ω,

$$\hat{d}[\Delta k(\Omega)] = \gamma L|d|\mathrm{sinc}\{[\Delta k(\Omega) - K_0]L/2\}, \quad (5.5)$$

and the k-vector mismatch is

$$\Delta k(\Omega) = 2k(\omega_1 + \Omega/2) - k(\omega_2 + \Omega) \quad (5.6)$$

or, by evaluation of the Taylor expansion up to the GVD terms in Eq. (5.6),

$$\Delta k(\Omega) = \Delta k_0 + \delta\nu\Omega + \frac{1}{2}\left(\frac{1}{2}\beta_1 - \beta_2\right)\Omega^2. \quad (5.7)$$

The result of Eq. (5.5) is a familiar cw SHG sinc tuning curve, whose width in the frequency space $\Delta\Omega_g$ is defined implicitly by $[\Delta k(\Delta\Omega_g) - K_0]L \sim 1$ and hence scales inversely with grating length L. There are two distinct regimes differentiated by the dimensionless parameter $\alpha = (\beta_1/2 - \beta_2)/(L\delta\nu^2)$. For small α, the behavior is dominated by the GVM term, and the GVD term causes some broadening and asymmetry of the tuning curve. The width of the tuning curve $\Delta\Omega_g$ [defined as the full width at half-maximum (FWHM) of the square of $\hat{d}(\Omega)$ given by Eq. (5.5)] is obtained, to second order in α, as

$$\Delta\Omega_g \approx \frac{5.57}{L|\delta\nu|}(1 + 3.87\alpha^2). \quad (5.8)$$

Figure 1(a) shows the tuning curves $|\hat{d}|^2$ as functions of normalized frequency $\Omega L\delta\nu$ for several values of α. In principle, when the grating k-vector is selected as $K_0 = \Delta k_0$ (QPM condition) the tuning curve as given by Eqs. (5.5) and (5.7) always has two peaks; one is at $\Omega = 0$, and the second is at $\Omega = -2\delta\nu/(\beta_1/2 - \beta_2)$. For small α, however, the second peak is far from the first, and typically its formally calculated spectral position is not at a frequency for which the Taylor expansion, Eq. (5.7), is valid.

When α increases, the second peak approaches the first one until they ultimately merge. The cross over between these two regimes occurs at $|\alpha| \approx 0.18$. For large α, the

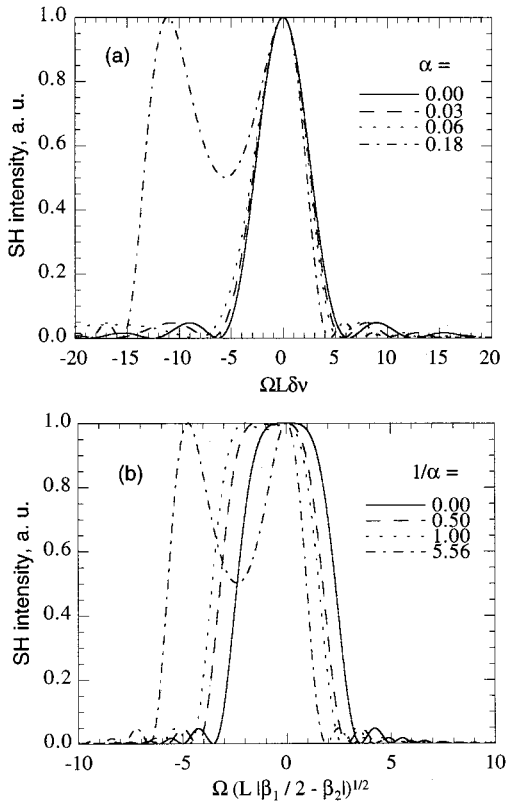

Fig. 1. Normalized cw tuning curves, $|\hat{d}|^2$, for a uniform grating in the presence of GVD for (a) small and (b) large values of $\alpha = (\beta_1/2 - \beta_2)/(L\delta\nu^2)$.

shape of the tuning curve is dominated by the GVD term, and its width is generally much broader than that in the small-α regime, leading to what is well known from the literature as wavelength-noncritical phase matching.[26,27] To first order in $1/\alpha$, $\Delta\Omega_g$ in this regime is obtained as

$$\Delta\Omega_g \approx \frac{4.72}{\sqrt{L|\beta_1/2 - \beta_2|}}\left(1 + \frac{0.090}{\alpha}\right). \tag{5.9}$$

Figure 1(b) shows the tuning curves $|\hat{d}|^2$ as functions of normalized frequency $\Omega\sqrt{L|\beta_1/2 - \beta_2|}$ for several values of $1/\alpha$.

6. LINEARLY CHIRPED GRATING AS A PULSE COMPRESSOR IN THE PRESENCE OF GROUP-VELOCITY DISPERSION AT THE SECOND HARMONIC

Let us consider a transform-limited FH Gaussian pulse with carrier frequency ω_1, $1/e$ intensity half-width τ_0, and amplitude E_0; its time-domain envelope is then

$$B_1(t) = E_0 \exp\left(-\frac{t^2}{2\tau_0^2}\right). \tag{6.1}$$

The frequency-domain envelope for such a pulse is then obtained from Eqs. (4.1) and (4.2) as

$$\hat{A}_1(\Omega) = \frac{1}{\sqrt{2\pi}} E_0 \tau_0 \exp\left(-\frac{1}{2}\tau_0^2 \Omega^2\right). \tag{6.2}$$

If this pulse is stretched in a linear delay line with GVD of C_1, it becomes linearly chirped; i.e., it acquires a quadratic-in-Ω phase, as can be obtained from Eq. (6.2) through Eq. (4.7):

$$\hat{A}_1(\Omega) = \frac{1}{\sqrt{2\pi}} E_0 \tau_0 \exp\left[-\frac{1}{2}(\tau_0^2 + iC_1)\Omega^2\right]. \tag{6.3}$$

The time-domain envelope of the chirped pulse is obtained by means of the inverse Fourier transform of Eq. (6.3) as

$$B_1(t) = E_0 \frac{\tau_0}{\sqrt{\tau_0^2 + iC_1}} \exp\left[-\frac{t^2}{2(\tau_0^2 + iC_1)}\right]. \tag{6.4}$$

The results of Eqs. (6.3) and (6.4) are well known from the literature.[4,6]

In Refs. 18 and 19 it was shown that, when GVD and higher-order dispersion at both the FH and the SH are negligible, the SH pulse generated in a linearly chirped grating has an additional linear chirp, relative to the input FH. More precisely, we considered a grating whose nonlinear coefficient distribution is given by

$$d(z) = |d| \exp\left[iK_0\left(z - \frac{L}{2}\right) + iD_g\left(z - \frac{L}{2}\right)^2\right] \mathrm{rect}\left(\frac{z}{L} - \frac{1}{2}\right), \tag{6.5}$$

where D_g is the grating chirp. The k-vector for this grating is obtained from Eq. (3.2) as

$$K(z) = K_0 + 2D_g\left(z - \frac{L}{2}\right), \tag{6.6}$$

which has a linear dependence on z.

The transfer function for this grating over the pulse bandwidth was obtained in Refs. 18 and 19 as

$$\hat{D}_0(\Omega) = \gamma|d| \sqrt{\frac{\pi}{D_g}} \exp\left(-i\frac{\delta\nu^2\Omega^2}{4D_g}\right), \tag{6.7}$$

as long as the grating length is selected to be long enough. $\hat{D}_0(\Omega)$ has a quadratic-in-Ω phase and hence imposes an additional linear chirp of $\delta\nu^2/2D_g$ on the SH, regardless of the shape of the input FH.

One obtains the necessary condition on the grating length such that the transfer function is accurately represented by Eq. (6.7) by noting that, for finite L, the amplitude of the transfer function has a characteristic top-hat profile, whose bandwidth $\Delta\Omega_g$ is obtained through the requirement that the k-vectors at the input and output of the grating be appropriate for phase matching (in the cw sense) of the $\pm\Delta\Omega_g/2$ frequency components, i.e., $|\Delta\Omega_g \delta\nu| = |K(L) - K(0)| = 2|D_g|L$. The phase of the transfer function over the range $|\Omega| \leqslant \Delta\Omega_g/2$ is still accurately represented by Eq. (6.7). If the grating length is selected such that $\Delta\Omega_g = 6/\tau_0$, then the SH pulse broadening due to the spectral truncation of the frequency components outside the $|\Omega| \leqslant \Delta\Omega_g/2$ range will be less than 10% (Ref. 19). Hence one obtains the condition for the necessary grating length as

$$L = \left|\frac{3\,\delta\nu}{D_g\tau_0}\right|. \tag{6.8}$$

If the input FH is a linearly chirped Gaussian pulse of the form of Eq. (6.3), and the grating chirp is selected as

$$D_g = -\frac{\delta\nu^2}{C_1}, \tag{6.9}$$

then from Eqs. (4.15), (4.16), and (6.7) we find that the generated SH will be transform limited.[18,19]

Since the GVD coefficient at the SH is typically several times larger than that at the FH (see Section 10), it is instructive to see how well a linearly chirped grating will perform as a compressor for the case in which a small amount of GVD at the SH is present but GVD at the FH is still negligible. The derivation of the proper grating function for compression when GVD at both SH and FH is present is given in Sections 7 and 8, where we find that when significant GVD at either SH or FH, or both, is present, the required grating has a more complicated, other than linear, chirp.

The transfer function for the linearly chirped grating of the form of Eq. (6.5) in the presence of GVD at the SH is obtained from Eqs. (4.12) and (4.17) as

$$\hat{D}_2 = \gamma|d| \sqrt{\frac{\pi}{D_g}} \exp\left[i\frac{1}{4}\beta_2 L\Omega^2 - i\frac{(\delta\nu\Omega - \beta_2\Omega^2/2)^2}{4D_g}\right]. \tag{6.10}$$

As is apparent from Eq. (6.10), the transfer function $\hat{D}_2(\Omega)$ for a linearly chirped grating in the presence of GVD at the SH has not only quadratic but also cubic and quartic phase terms. For a Gaussian linearly chirped FH pulse of the form of Eq. (6.3), we obtain the Fourier transform of the output SH time-domain envelope by substituting Eq. (6.10) into Eq. (4.18) and using Eqs. (4.1) and (4.2):

$$\hat{B}_2(L,\Omega) \propto \exp\left[-\frac{1}{4}\tau_0^2\Omega^2 - \frac{i}{4}\left(C_1 + \beta_2 L + \frac{\delta\nu^2}{D_g}\right)\Omega^2 + \frac{i}{4}\frac{\delta\nu\beta_2}{D_g}\Omega^3 - \frac{i}{16}\frac{\beta_2^2}{D_g}\Omega^4\right]. \tag{6.11}$$

As can be seen from relation (6.11), when $\beta_2 \neq 0$, regardless of the choice of grating chirp D_g, the SH pulse generated in a linearly chirped grating will always have some uncompensated phase; i.e., this pulse will not be transform limited. We can set to zero the quadratic-in-Ω phase factor in relation (6.11) by selecting the grating chirp as

$$D_g = -\frac{\delta\nu^2}{C_1 + \beta_2 L}. \tag{6.12}$$

The remaining Ω^3- and Ω^4-phase terms will lead to uncompensated SH pulse broadening. Equation (6.12) can be inverted to yield the FH chirp needed to generate a SH with zero quadratic phase in a grating with given D_g:

$$C_1 = -\frac{\delta\nu^2}{D_g} - \beta_2 L, \tag{6.13}$$

or, if the grating length is selected according to Eq. (6.8),

$$C_1 = -\frac{\delta\nu^2}{D_g}\left(1 + \frac{3\beta_2}{\delta\nu\tau_0}\right). \tag{6.14}$$

So inclusion of GVD at the SH leads to a shift of the optimum FH chirp for compression in a grating with given D_g, as well as to some broadening of the SH (as compared with the non-GVD case), owing to the Ω^3- and Ω^4-phase terms. Elimination of these terms requires a nonlinearly chirped QPM grating, as discussed in Sections 7 and 8.

We numerically calculated the temporal profile of the SH pulse by using the inverse Fourier transform of Eq. (6.11) and evaluated its 1/*e* intensity full width $2\tau_2$. Figure 2 shows the dependence of the normalized SH pulse length τ_2/τ_0 as a function of normalized FH chirp C_1/τ_0^2 for several values of normalized GVD coefficient at the SH, $\beta_2/\delta\nu\tau_0$. A normalized grating chirp $D_g(\tau_0/\delta\nu)^2 = -0.1$ is assumed. With increasing β_2 the optimum FH chirp shifts from its value for $\beta_2 = 0$, as predicted by Eq. (6.14), and the minimum SH pulse length increases as the contribution of the Ω^3- and Ω^4-phase terms in relation (6.11) increases with β_2. We also note that there is a sizable range of the FH chirp, ΔC_1, over which the SH pulse length is relatively constant. When C_1 is slightly detuned from its optimum value [given by Eq. (6.14)], the SH envelope has nonzero quadratic phase, which, however, does not contribute to significant pulse broadening until it is larger than the contribution of the Ω^3- and Ω^4-phase terms. This range is estimated as

$$\Delta C_1 \approx 6\left|\frac{\delta\nu^2}{D_g}\frac{\beta_2}{\delta\nu\tau_0}\right|, \tag{6.15}$$

which is in agreement with the results shown in Fig. 2. We also note that jumps in the SH pulse length, which are apparent for larger values of β_2, are due to the fact that the Ω^3-phase term in relation (6.11) leads to the ripples in the pulse shape[4,6] and consequently causes the stepwise increase in the pulse length, which is evaluated at the constant level of 1/*e*.

To quantify the amount of pulse broadening that is due to the Ω^3- and Ω^4-phase terms in relation (6.11) we calculated the SH pulse length under the assumption that the FH chirp is selected according to Eq. (6.14) to compensate for the quadratic phase. We are interested in the regime in which the broadening caused by β_2 is relatively small. In this regime the nonquadratic phase is dominated by the cubic term in relation (6.11), and we neglect the contribution of the Ω^4-phase term. We calculated the normalized SH 1/*e* intensity full width $2\tau_2$, as shown in Fig. 3, where τ_2/τ_0 is plotted as a function of

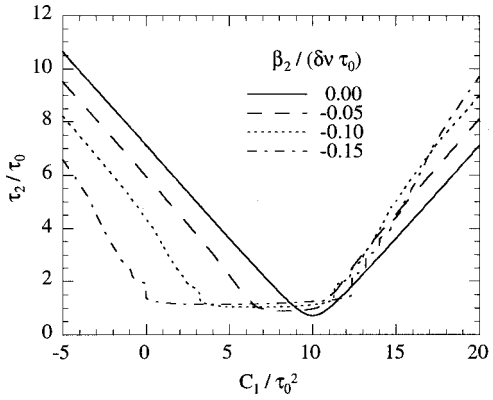

Fig. 2. Dependence of the normalized SH pulse length τ_2/τ_0 as a function of normalized FH chirp C_1/τ_0^2 for several values of normalized GVD coefficient at the SH, $\beta_2/\delta\nu\tau_0$. A linearly chirped grating with length as given by Eq. (6.8) and with a normalized chirp $D_g(\tau_0/\delta\nu)^2 = -0.1$ is assumed.

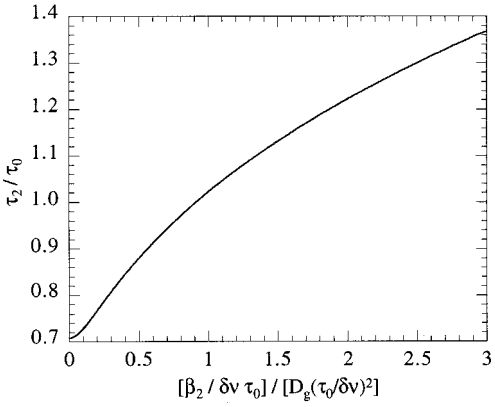

Fig. 3. Effect of uncompensated cubic phase on the length of the SH pulse generated in a linearly chirped grating in the presence of GVD at the SH. The normalized SH pulse length τ_2/τ_0 obtained from relation (6.11) when the FH chirp is selected according to Eq. (6.14) is plotted as a function of $(\beta_2/\delta\nu\tau_0)/[D_g(\tau_0/\delta\nu)^2]$.

$(\beta_2/\delta\nu\tau_0)/[D_g(\tau_0/\delta\nu)^2]$. We can see that the SH pulse length exceeds that of the FH when such normalized β_2 exceeds ~1.

7. ENGINEERING OF THE GRATING *k*-VECTOR FOR ARBITRARY PULSE PHASES IN THE PRESENCE OF ARBITRARY DISPERSION

As was pointed out in Section 4, the advantage of the transfer function relations of Eqs. (4.15) and (4.18) is that they trivially enable one to design the grating function $d(z)$ necessary to perform the desired pulse shaping transformation for arbitrary pulse shapes. However, if the GVD at the FH becomes significant, one has to use Eq. (4.8), which does not provide a ready way for such a design of $d(z)$. In this section, by assuming that the conversion is localized at a point and using an intuitive frequency-domain analysis, we develop a procedure, valid for arbitrary material dispersion, for the design of the grating k-vector necessary to compensate for arbitrary FH phase to generate a SH pulse with a desired phase distribution. Strictly speaking, the conversion is never localized at a point but is always spread over a range of grating k-vectors, the effect of which can accurately be handled in strongly chirped gratings by the method of stationary phase, which provides mathematical justification for the heuristic approach. The results obtained in this section agree with the exact calculations for a particular case of Gaussian pulses and no dispersion beyond GVD, presented in Section 8, as well as with numerical modeling, presented in Section 9.

The evolution of the phase of a general FH pulse when it propagates through the QPM grating shall be considered first. Since the conversion is driven by the nonlinear polarization, which is proportional to the square of the FH in the time domain (or to the FH self-convolution in the frequency domain), we derive a propagation law, for the phase of the nonlinear polarization, that in general is different from that of the FH. A particular frequency component of the nonlinear polarization accumulates a certain phase shift in traveling from the input of the grating to a location where the conversion of this component is phase matched, and then, after the conversion, the generated SH component travels toward the output of the grating, accumulating a certain phase shift, as governed by the SH phase propagation law. By specifying the desired phase of the SH pulse as a function of frequency at the output, we obtain the grating locations where different components have to be converted and subsequently derive the necessary grating phase distribution.

Consider a FH pulse with spectrum $\hat{E}_1(z=0,\omega)$ input to the QPM grating. This pulse propagates through the dispersive medium according to Eq. (4.7) as

$$\hat{E}_1(z,\omega) = \hat{E}_1(z=0,\omega)\exp[-ik(\omega)z]. \tag{7.1}$$

Hence in the frequency domain the dispersive propagation over distance z results in the position-dependent phase distribution of different frequency components, Φ_{FH}:

$$\begin{aligned}\Phi_{\mathrm{FH}} &= \Phi_1(\Omega_1) - k(\omega_1+\Omega_1)z \\ &= \Phi_1 - k_1 z - (z/u_1)\Omega_1 - \tilde{k}_1(\Omega_1)z,\end{aligned} \tag{7.2}$$

where the FH pulse phase at the input to the grating is $\Phi_1(\Omega_1) = \angle[\hat{E}_1(0,\omega_1+\Omega_1)]$, $\angle[x]$ denotes the phase of a complex quantity x, and $\tilde{k}_i(\Omega_i)$ contains GVD and higher-order terms in the Taylor expansion of $k(\omega_i+\Omega_i)$:

$$\tilde{k}_i(\Omega_i) = \sum_{n=2}^{\infty}\frac{1}{n!}\left[\frac{\mathrm{d}^n k(\omega)}{\mathrm{d}\omega^n}\right]\Bigg|_{\omega=\omega_i}\Omega_i^n. \tag{7.3}$$

The SH conversion is driven by the nonlinear polarization, whose spectrum is proportional to the product of the nonlinear coefficient and a self-convolution of the FH pulse spectrum, i.e., $\hat{P}_{\mathrm{NL}}(z,\omega) = \varepsilon_0 d(z)\int_{-\infty}^{+\infty}\hat{E}_1(z,\omega')\hat{E}_1(z,\omega-\omega')\mathrm{d}\omega'$, Ref. 28, and hence can be written from Eqs. (7.1) and (7.2) as

$$\hat{P}_{\mathrm{NL}}(z,\Omega) = \varepsilon_0 d(z)\exp[-2ik_1 z - i(z/u_1)\Omega]\hat{p}(z,\Omega), \tag{7.4}$$

where $\hat{p}$ is

$$\begin{aligned}\hat{p}(z,\Omega) = \int_{-\infty}^{+\infty}&\hat{E}_1(0,\omega_1+\Omega')\hat{E}_1(0,\omega_1+\Omega-\Omega') \\ &\times\exp[-i\tilde{k}_1(\Omega')z - i\tilde{k}_1(\Omega-\Omega')z]\mathrm{d}\Omega',\end{aligned} \tag{7.5}$$

with $\Omega' = \omega' - \omega_1$. We notice that, in the absence of GVD and higher-order material dispersion ($\tilde{k}_1 = 0$), $\hat{p}$ is just the z-invariant self-convolution of the input FH field, so the nonlinear polarization propagates with the same group velocity as the FH itself, and hence the propagation laws for the phases of $\hat{P}_{\mathrm{NL}}$ and $\hat{E}_1$ are the same. However, when GVD is present the rates at which $\hat{P}_{\mathrm{NL}}$ and $\hat{E}_1$ disperse are in general different. Moreover, for $\hat{P}_{\mathrm{NL}}$ the phase propagation law depends on the shape of the input FH pulse, as is apparent from Eq. (7.5), which has to be known if one is to obtain a simple algebraic form similar to Eq. (7.2). This distinction between $\hat{P}_{\mathrm{NL}}$ and $\hat{E}_1$ is what makes the problem complicated.

Let us consider a particular frequency component Ω_0 of the nonlinear polarization and assume that it converts to the SH at a location z_0 in the QPM grating. By traveling from $z=0$ to $z=z_0$ this component accumulates a particular phase shift Φ_P, which is obtained from Eqs. (7.4) and (7.5) as

$$\Phi_P = \Phi(z_0) - 2k_1 z_0 - (z_0/u_1)\Omega_0 + \angle[\hat{p}(z_0,\Omega_0)], \tag{7.6}$$

where $\Phi(z_0)$ is the phase of $d(z)$ at the location $z=z_0$ [see Eq. (3.1)]. After conversion at $z=z_0$ this frequency component propagates as a SH component, hence accumulating a certain phase, which is obtained, similarly to Eq. (7.2), as

$$\begin{aligned}\Phi_{\mathrm{SH}} &= -k(\omega_2+\Omega_0)(L-z_0) \\ &= -k_2(L-z_0) - [(L-z_0)/u_2]\Omega_0 \\ &\quad - \tilde{k}_2(\Omega_0)(L-z_0).\end{aligned} \tag{7.7}$$

The total phase that this Ω_0 component has at the output of the grating, Φ_{total}, is the sum of Φ_P and Φ_{SH} and is obtained from Eqs. (7.6) and (7.7) as

$$\Phi_{\text{total}}(z_0, \Omega_0) = \Phi(z_0) - \Delta k_0 z_0 - k_2 L - \delta\nu z_0 \Omega_0 - (L/u_2)\Omega_0 + \angle[\hat{p}(z_0, \Omega_0)] - \tilde{k}_2(\Omega_0)(L - z_0). \quad (7.8)$$

The grating has to be designed such that this total phase Φ_{total} is equal to the desired phase of the SH, $\Phi_2(\Omega_0)$, which is to be generated at the output of the grating; i.e., we find $\Phi(z_0)$ such that $\Phi_2(\Omega_0) = \Phi_{\text{total}}(\Omega_0)$. To specify the location z_0 at which the Ω_0 component must be converted, we require that the conversion location be selected such that the group delay, which can be obtained by differentiation of Φ_{total} with respect to Ω_0, must equal the desired group delay, $\partial\Phi_2/\partial\Omega_0$, for all Ω_0, i.e., $\partial\Phi_2/\partial\Omega_0 - \partial\Phi_{\text{total}}/\partial\Omega_0 = 0$. Using Eq. (7.8), we obtain

$$\frac{\partial}{\partial\Omega_0}\Phi_2(\Omega_0) + \delta\nu z_0 + \frac{L}{u_2} - \frac{\partial}{\partial\Omega_0}\angle[\hat{p}(z_0, \Omega_0)] + (L - z_0)\frac{\partial}{\partial\Omega_0}\tilde{k}_2(\Omega_0) = 0. \quad (7.9)$$

Solving Eq. (7.9) gives the functional dependence $\Omega_0 = \Omega_0(z_0)$, which specifies the component Ω_0 that is to be converted at the location z_0. Substituting $\Omega_0(z_0)$ into Eq. (7.8) and setting $\Phi_{\text{total}}(\Omega_0) = \Phi_2(\Omega_0)$ allows elimination of Ω_0 and yields the necessary grating phase $\Phi = \Phi(z_0)$.

The intuitive frequency-domain grating design procedure described above can be put into more mathematically rigorous form by the method of stationary phase for asymptotic evaluation of integrals with rapidly oscillating integrands.[29,30] The general result for the output SH field, valid for arbitrary dispersion and pulse shapes, Eqs. (4.8)–(4.10), can be rewritten as

$$\hat{E}_2(L, \omega_2 + \Omega) = -i\gamma \exp[-ik(\omega_2 + \Omega)L] \times \int_{-\infty}^{+\infty} |d(z)| \exp[i\Phi(z)]\hat{p}(z, \Omega) \times \exp(-i\Delta k_0 z - i\delta\nu\Omega z) \times \exp[i\tilde{k}_2(\Omega)z]\mathrm{d}z, \quad (7.10)$$

where $\hat{p}(z,\Omega)$ is defined by Eq. (7.5) and $\tilde{k}_2(\Omega)$ is defined by Eq. (7.3). One obtains the leading behavior of the integral in Eq. (7.10) by the method of stationary phase by realizing that the main contribution to the integral comes from the region around point z_0, where the phase variation of the integrand is slowest, i.e., $\Phi'(z_0) + \angle[\hat{p}(z_0, \Omega)] - \Delta k_0 - \delta\nu\Omega + \tilde{k}_2(\Omega) = 0$. Applying the standard stationary phase result[29,30] yields

$$\hat{E}_2(L, \omega_2 + \Omega) = -i\gamma|d(z_0)||\hat{p}(z_0, \Omega)| \times \left(\frac{2\pi}{|\Phi''(z_0) + \{\angle[\hat{p}(z_0, \Omega)]\}''|}\right)^{1/2} \times \exp[i\Phi_{\text{total}}(z_0, \Omega)], \quad (7.11)$$

where $\Phi_{\text{total}}(z_0, \Omega)$ is the same as defined by Eq. (7.8). We note that the conversion efficiency of different frequency components is affected both by the spreading of the FH, which is due to GVD and higher-order dispersion, as represented by the $\hat{p}(z_0, \Omega)$ factor in Eq. (7.11), and by the second derivative of the necessary phase of the grating.

Since the expression for the total phase in Eq. (7.11) is the same as that of the heuristic point conversion picture, Eq. (7.8), we can also view this result as a first-order justification for that picture and would of course find the same result for the required grating phase $\Phi(z)$, as in Eq. (7.9). The rigorous estimation of the accuracy of the stationary phase approximation of the integral in Eq. (7.10) with its leading behavior, Eq. (7.11), is complicated and requires delicate estimation of integrals. In principle, higher-order terms in the asymptotic expansion can be estimated by the method of steepest descent.[29,30] The physically intuitive condition for applicability of the stationary phase method is that the distance over which the conversion is phase matched, as determined by the inverse of the factor $\Phi''(z) \equiv K'(z)$ in Eq. (7.11), must be much smaller than the grating length designed to accommodate conversion of all frequency components, or, in other words, the required grating must be strongly chirped, $K'(z)L^2 \gg 1$ for all $z \in [0, L]$.

As a particular example of the application of this grating design procedure we consider generation of a linearly chirped SH pulse from a Gaussian linearly chirped FH pulse of the form of Eq. (6.3) for the case in which dispersion terms beyond GVD can be neglected, i.e., $\tilde{k}_i(\Omega) = (1/2)\beta_i\Omega^2$. In this case Eq. (7.5) can be integrated analytically in closed form, resulting in

$$\Phi_P = \Phi(z_0) - \frac{1}{2}\arctan\left(\frac{C_1 + \beta_1 z_0}{\tau_0^2}\right) - 2k_1 z_0 - \frac{z_0}{u_1}\Omega_0 - \frac{1}{4}(C_1 + \beta_1 z_0)\Omega_0^2. \quad (7.12)$$

The phase that Ω_0 accumulates by propagating as a SH component is obtained from Eq. (7.7) as

$$\Phi_{\text{SH}} = -k_2(L - z_0) - \frac{L - z_0}{u_2}\Omega_0 - \frac{1}{2}\beta_2\Omega_0^2(L - z_0). \quad (7.13)$$

The desired phase of the SH pulse at the output is

$$\Phi_2 = -\left(\frac{L}{u_1} - \Delta T\right)\Omega_0 - \frac{1}{2}C_2\Omega_0^2, \quad (7.14)$$

which has a chirp of C_2 and is delayed by ΔT relative to the FH pulse. We note that the grating length L and the delay ΔT, treated here as parameters, have to be selected properly in the manner described in Section 8.

Substituting Eqs. (7.12) and (7.13) into Eq. (7.8) and differentiating Eq. (7.9), we obtain an implicit relation for the location z_0 at which frequency component Ω_0 should be converted:

$$\Omega_0 = 2\frac{\delta\nu(L - z_0) - \Delta T}{C(z_0)}, \quad (7.15)$$

where

$$C(z) = C_1 - 2C_2 + (\beta_1 - 2\beta_2)z + 2\beta_2 L. \quad (7.16)$$

The grating phase is then obtained from Eq. (7.8) with Eq. (7.15) as

$$\Phi(z_0) = \frac{1}{2}\arctan\left(\frac{C_1 + \beta_1 z_0}{\tau_0^2}\right) + \Delta k_0 z_0 - \frac{[\delta\nu(L - z_0) - \Delta T]^2}{C(z_0)}, \quad (7.17)$$

where we neglected a constant phase term.

The result of the stationary phase method, Eq. (7.11), also predicts amplitudes of the different spectral components of the generated SH pulse. Using Eq. (7.11) with the result of Eq. (7.17) and analytically evaluating $\hat{p}(z, \Omega)$, Eq. (7.5), for the case of Gaussian pulses and negligible dispersion beyond GVD, we obtain the necessary modulation of the grating amplitude for uniform conversion of different components:

$$|d(z)| \propto \left[\frac{1}{\pi|C(z)|}\frac{\tau_1(z)}{\tau_0}\right]^{1/2}\left|\delta\nu + (\beta_1 - 2\beta_2)\frac{\delta\nu(L - z) - \Delta T}{C(z)}\right|, \quad (7.18)$$

where the z-dependent length of the FH pulse is

$$\tau_1(z) = \{\tau_0^2 + [C_1(z)/\tau_0]^2\}^{1/2}. \quad (7.19)$$

The results obtained for the required grating phase, Eq. (7.17), and grating amplitude modulation, relation (7.18), are exactly the same as the ones obtained from the rigorous analysis presented in Section 8 for the particular case of Gaussian pulses and negligible dispersion beyond GVD [see Eqs. (8.10) and (8.11)].

8. CHIRPED GRATING COMPRESSOR IN THE PRESENCE OF GROUP-VELOCITY DISPERSION AT BOTH THE SECOND HARMONIC AND THE FIRST HARMONIC

In this section we consider a restricted class of linearly chirped Gaussian FH pulses and neglect dispersion beyond GVD at the FH, i.e., $\delta k''(\Omega, \Omega') = 0$ in Eq. (4.13). We find that in this case one can integrate, in a closed form, the integral expression for the output SH envelope, Eq. (4.8), to obtain a relation similar to the transfer function relations of Eqs. (4.15) and (4.18). Furthermore, neglecting the dispersion terms higher than GVD at the SH, i.e., $\delta k'(\Omega) = 0$ in Eq. (4.12), we derive an analytical expression for $d(z)$ that is necessary for the generation of a linearly chirped SH pulse. The result for the grating phase is the same as that of Section 7, Eq. (7.17); however, in the derivation of this section we do not make any mathematical approximations.

Assuming an input linearly chirped Gaussian FH pulse with a frequency-domain envelope as given by Eq. (6.3), substituting it into Eqs. (4.8)–(4.13), and carrying out integration over Ω', we obtain

$$\hat{A}_2(L, \Omega) = -i\gamma\widehat{A_1^2}(\Omega)\int_{-\infty}^{+\infty} dz\,\tilde{d}(z)\exp[-i\mu(\Omega)z], \quad (8.1)$$

where we have defined

$$\mu(\Omega) = \Delta k'(\Omega) - \frac{1}{4}\beta_1\Omega^2 = \Delta k_0 + \delta\nu\Omega + \frac{1}{2}\left(\frac{1}{2}\beta_1 - \beta_2\right)\Omega^2 + \delta k'(\Omega), \quad (8.2)$$

$$\tilde{d}(z) = d(z)\left[\frac{\tau_0^2 + iC_1}{\tau_0^2 + iC_1(z)}\right]^{1/2} \quad (8.3)$$

with the z-dependent chirp of the FH pulse being defined as

$$C_1(z) = C_1 + \beta_1 z, \quad (8.4)$$

where C_1 is the chirp of the FH pulse at the input to the grating [see Eq. (6.3)]. $\delta k'(\Omega)$ is as defined in Eq. (4.12), and $\widehat{A_1^2}(\Omega)$ is a self-convolution [Eq. (4.16)] of the Gaussian FH pulse envelope, Eq. (6.3).

The integral in Eq. (8.1) is proportional to the Fourier transform of $\tilde{d}(z)$ with the transform variable μ. Equation (8.1) does not have the form of a transfer function relation, since $\tilde{d}(z)$ depends on the parameters of the input FH pulse, viz., its initial chirp and pulse length. Comparing the transfer function relation, Eq. (4.18), with Eq. (8.1), we note that the latter is valid for a restricted class of FH pulses, i.e., linearly chirped Gaussians, not arbitrary FH pulses, but that the dispersion at the FH is included up to the GVD in Eq. (8.1), whereas Eq. (4.18) was obtained when we neglected GVD and higher-order dispersion at the FH. We also recall that both Eqs. (8.1) and (4.18) are valid for arbitrary dispersion at the SH.

The grating function $d(z)$ necessary to generate a desired SH pulse from a given Gaussian FH pulse is obtained from Eq. (8.1) by use of the inverse Fourier transform as

$$d(z) = i\frac{1}{2\pi\gamma}\left[\frac{\tau_0^2 + iC_1(z)}{\tau_0^2 + iC_1}\right]^{1/2} \times \int_{-\infty}^{+\infty} d\mu\,\frac{\hat{A}_2(L, \Omega)}{\widehat{A_1^2}(\Omega)}\exp[i\mu(\Omega)z], \quad (8.5)$$

where Ω is considered to be a function of μ as can be obtained by inversion of Eq. (8.2). We stress again that in Eq. (8.5) the FH is a linearly chirped Gaussian pulse, not an arbitrary pulse; however, we did not make any assumptions about the shape or chirp of the SH pulse, which can be arbitrary. Hence Eq. (8.5) gives an explicit prescription for the design of a QPM grating for the generation of a shaped SH pulse from a Gaussian FH pulse.

The integral in Eq. (8.5) can be evaluated analytically for a technologically important particular case of pulse shaping: generation of a Gaussian linearly chirped SH pulse (or transform-limited SH pulse, as a special case when chirp is equal to zero), when dispersion beyond GVD at not only the FH but also the SH can be neglected, i.e., $\delta k'(\Omega) = 0$ in Eq. (4.12). The Fourier transform of

the time-domain envelope of an output Gaussian SH pulse of width τ_2, chirp C_2, and amplitude E_{20} is given by

$$\hat{B}_2(L,\Omega) = \frac{1}{\sqrt{2\pi}} E_{20}\tau_2 \times \exp\left[-\frac{1}{2}(\tau_2^2 + iC_2)\Omega^2 - i\left(\frac{L}{u_1} - \Delta T\right)\Omega\right]. \tag{8.6}$$

The linear-in-Ω factor in Eq. (8.6) indicates that the desired SH pulse is delayed from the FH pulse at the output of the grating by ΔT, as can be verified by comparison of the Fourier transform of the output time-domain envelope for the Gaussian FH pulse. The frequency-domain envelope for the SH pulse is obtained from Eq. (8.6) as

$$\hat{A}_2(L,\Omega) = \frac{1}{\sqrt{2\pi}} E_{20}\tau_2 \exp\left[-\frac{1}{2}(\tau_2^2 + iC_2 - i\beta_2 L)\Omega^2 - i(\delta\nu L - \Delta T)\Omega\right]. \tag{8.7}$$

The desired value of the delay ΔT will be specified below.

Since the QPM grating acts like a filter, and not like an amplifier, in the frequency domain, it cannot provide significant bandwidth enhancement without significant attenuation of the central spectral components. Hence we choose the spectral width of the SH to be the same as that of $\widehat{A_1^2}$; from Eqs. (4.16), (6.3), and (8.7) we obtain

$$\tau_2 = \tau_0/\sqrt{2}. \tag{8.8}$$

We also note that the amplitude of the SH pulse, E_{20}, cannot be arbitrarily high since its upper bound is set by the available nonlinearity. The maximum possible value for E_{20} will be obtained below [see Eq. (8.19)].

Substituting Eqs. (4.16), (6.3), (8.7), and (8.8) into Eq. (8.5) and integrating, we obtain the desired grating function as

$$d(z) = |d(z)|\exp[i\Phi(z)], \tag{8.9}$$

where the z-dependent phase of the grating, $\Phi(z)$, is

$$\Phi(z) = \frac{1}{2}\arctan\left[\frac{C_1(z)}{\tau_0^2}\right] + \Delta k_0 z - \frac{[\delta\nu(L-z) - \Delta T]^2}{C(z)} \tag{8.10}$$

and the z-dependent grating amplitude is

$$|d(z)| = \frac{1}{\gamma}\frac{E_{20}}{E_0^2}\left[\frac{1}{\pi|C(z)|}\frac{\tau_1(z)}{\tau_0}\right]^{1/2}\left|\delta\nu + (\beta_1 - 2\beta_2)\frac{\delta\nu(L-z) - \Delta T}{C(z)}\right|, \tag{8.11}$$

where the z-dependent length of the FH pulse, $\tau_1(z)$, is as defined by Eq. (7.19) and $C(z)$ is as defined by Eq. (7.16).

The z-dependent k-vector of the grating is the derivative of the grating phase $\Phi(z)$ given by Eq. (8.10):

$$K(z) = \frac{1}{2}\beta_1\frac{1}{\tau_1^2(z)} + \Delta k_0 + 2\delta\nu\frac{\delta\nu(L-z) - \Delta T}{C(z)} + (\beta_1 - 2\beta_2)\frac{[\delta\nu(L-z) - \Delta T]^2}{C(z)^2}. \tag{8.12}$$

This analysis and the resulting expressions are valid for the case in which the GVD is considered to be a correction to the GVM; more precisely, it works when $L_{gv} \ll L_{\beta 1}, L_{\beta 2}$. Otherwise, the GVD-induced pulse spreading is comparable with or greater than pulse walk-off. It turns out that, for common QPM ferroelectrics, the condition $L_{gv} \ll L_{\beta 1}, L_{\beta 2}$ is satisfied for pulses longer than ~5 fs at wavelengths shorter than the group-velocity degeneracy points, $\lambda_1 < 2\ \mu$m (see Section 10).

Note that we have not yet specified the time delay ΔT between the FH and the SH pulses at the output of the grating, as well as the grating length L. These parameters have to be selected properly to avoid bandwidth truncation; i.e., the grating bandwidth $\Delta\Omega_g$ has to be equal to $6/\tau_0$. In a manner similar to the selection of the appropriate length of a linearly chirped grating in the negligible-GVD case, described in Section 6, we require that ΔT and L, which appear as parameters in Eq. (8.12), be chosen such that the grating k-vectors at the input, $K(0)$, and at the output to the grating, $K(L)$, phase match (in the cw sense) frequencies $\pm\Delta\Omega_g/2$. Explicitly, the conditions are obtained from Eq. (5.7) as

$$K(0) = \Delta k_0 \pm \delta\nu\frac{\Delta\Omega_g}{2} + \frac{1}{2}\left(\frac{1}{2}\beta_1 - \beta_2\right)\left(\frac{\Delta\Omega_g}{2}\right)^2, \tag{8.13}$$

$$K(L) = \Delta k_0 \mp \delta\nu\frac{\Delta\Omega_g}{2} + \frac{1}{2}\left(\frac{1}{2}\beta_1 - \beta_2\right)\left(\frac{\Delta\Omega_g}{2}\right)^2. \tag{8.14}$$

From Eq. (8.12), $K(L) > K(0)$ when $C_1 - 2C_2 < 0$, and $K(L) < K(0)$ when $C_1 - 2C_2 > 0$. Hence in Eqs. (8.13) and (8.14) the upper sign is chosen when $(C_1 - 2C_2)\delta\nu > 0$ and the lower sign is chosen otherwise.

We obtain the required delay ΔT as a function of crystal length L and pulse parameters by substituting Eq. (8.12) into the set of Eqs. (8.13) and (8.14) and eliminating $\Delta\Omega_g$:

$$\Delta T = \frac{1}{2}\delta\nu L\frac{C_1 - 2C_2 + \beta_1 L}{C_1 - 2C_2 + (\beta_1 + 2\beta_2)L/2}. \tag{8.15}$$

In the derivation of this expression for ΔT we have neglected the first term in the expression for $K(z)$, Eq. (8.12), since its contribution is small and its inclusion produces a much more complicated expression for ΔT. We then obtain the required length of the grating L from Eq. (8.13) by eliminating $\Delta\Omega_g = 6/\tau_0$ and using Eq. (8.15) for ΔT, as

$$L = \frac{3|C_1 - 2C_2|/\tau_0}{|\delta\nu| \pm (3/2)[(\beta_1 + 2\beta_2)/\tau_0]}, \tag{8.16}$$

where the plus sign in the denominator is chosen when $C_1 - 2C_2 < 0$ and the minus sign is chosen otherwise. Figure 4 shows the required grating length given by Eq. (8.16) normalized to the grating length for the case in

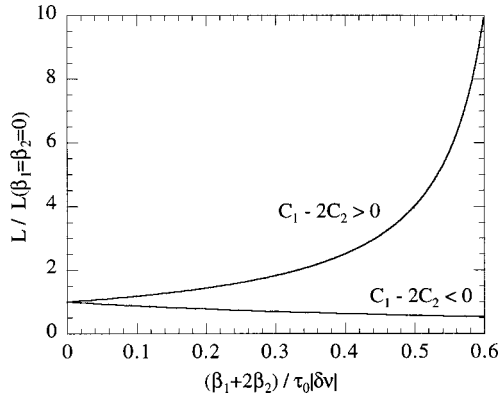

Fig. 4. Required length of a chirped grating, as given by Eq. (8.16), normalized to the grating length for the case $\beta_1 = \beta_2 = 0$, as a function of $(\beta_1 + 2\beta_2)/\tau_0|\delta\nu|$. The two branches correspond to the two signs in the denominator of Eq. (8.16).

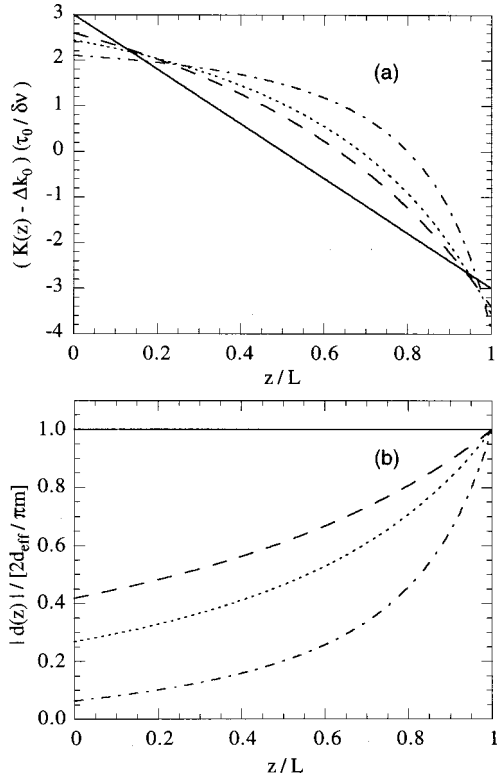

Fig. 5. (a) Normalized grating k-vector, $[K(z) - \Delta k_0](\tau_0/\delta\nu)$, as obtained with Eq. (8.12), and (b) normalized grating amplitude, $|d(z)|$, as obtained with Eq. (8.11). Both are plotted as functions of normalized position in the grating, z/L, for several representative pairs of the normalized GVD coefficients, $(\beta_1/\delta\nu\tau_0, \beta_2/\delta\nu\tau_0)$: solid curve (0, 0); dashed curve, (0.02, 0.10); dotted curve, (0.05, 0.15); dotted–dashed curve, (0.10, 0.25).

which $\beta_1 = \beta_2 = 0$ as a function of $(\beta_1 + 2\beta_2)/\tau_0|\delta\nu|$. The two branches correspond to different signs in the denominator of Eq. (8.16).

Figure 5(a) shows the normalized grating k-vector necessary to generate a compressed SH pulse ($C_2 = 0$) from a Gaussian FH pulse with the normalized chirp $C_1/\tau_0^2 = 10$ for several values of the normalized GVD coefficients $\beta_1/(\tau_0\delta\nu)$ and $\beta_2/(\tau_0\delta\nu)$. When the GVD is negligible at both the SH and the FH, i.e., $\beta_1 = \beta_2 = 0$, then from Eq. (8.15) the delay is $\Delta T = \delta\nu L/2$ and from Eq. (8.16) the grating length is $L = |3C_1/\tau_0\delta\nu|$, in agreement with Eqs. (6.8) and (6.9). The grating k-vector as obtained from Eq. (8.12) is linear with z, $K(z) = \Delta k_0 - 2(\delta\nu^2/C_1)(z - L/2)$, in agreement with previously derived results, Eqs. (6.5)–(6.9). As is apparent from Fig. 5(a), with increasing β_1 and β_2, $K(z)$ deviates from the linear behavior and acquires significant curvature.

In the expression for the modulated amplitude of the grating, Eq. (8.11), the amplitude of the generated SH wave, E_{20}, is not an independent parameter because the upper bound on $|d(z)|$ is set by the available nonlinearity, $|d(z)| \leqslant (2/\pi m)d_{\text{eff}}$ (see Section 3). Under the condition $L_{\text{gv}} \ll L_{\beta 1}, L_{\beta 2}$, the grating amplitude, as given by Eq. (8.11), is a monotonic function over the grating length, and hence it achieves its maximum value of $(2/\pi m)d_{\text{eff}}$ at either $z = 0$ or $z = L$. Equation (8.11) can then be rewritten as

$$|d(z)| = \frac{2}{\pi m}\frac{d_{\text{eff}}}{M}\left[\frac{\tau_0\tau_1(z)}{|C(z)|}\right]^{1/2}\frac{1}{|\delta\nu|}\left|\delta\nu + (\beta_1 - 2\beta_2)\frac{\delta\nu(L - z) - \Delta T}{C(z)}\right|, \quad (8.17)$$

where the scaling constant M is

$$M = \max\left\{\left[\frac{\tau_0\tau_1(0)}{|C(0)|}\right]^{1/2}\left|\frac{2C(L)}{C(0) + C(L)}\right|, \left[\frac{\tau_0\tau_1(L)}{|C(L)|}\right]^{1/2}\left|\frac{2C(0)}{C(0) + C(L)}\right|\right\}. \quad (8.18)$$

The amplitude of the generated SH pulse, E_{20}, is then obtained as

$$E_{20} = \frac{2}{\sqrt{\pi}m}\frac{d_{\text{eff}}}{M}L_{\text{gv}}\gamma E_0^2. \quad (8.19)$$

Figure 5(b) shows $|d(z)|$ normalized to $(2/\pi m)d_{\text{eff}}$ for the same set of the normalized GVD coefficients $\beta_1/(\tau_0\delta\nu)$ and $\beta_2/(\tau_0\delta\nu)$ as in Fig. 5(a). We note that $|d(z)|$ increases as the curvature of $K(z)$ increases, in agreement with the result of the stationary phase analysis of Section 7, Eq. (7.11). Since the conversion of a particular frequency component occurs over a finite range of grating k-vectors and since $dK(z)/dz$ is not constant for nonlinearly chirped gratings, the distance over which a particular frequency component is phase matched also varies, leading to different efficiencies for different frequency components, which must be compensated by the modulation of the grating amplitude. The GVD-induced spreading of the FH pulse, and hence the reduction of the peak power, are other effects that require compensation by the grating amplitude; both are accounted for in Eq. (8.17).

Equations (8.9), (8.10), and (8.15)–(8.18) completely specify the grating function that is necessary to generate a Gaussian SH pulse with a desired linear chirp from a Gaussian FH pulse with a given chirp, valid for up to the GVD dispersion terms at both the FH and the SH.

9. NUMERICAL MODELING

From the theoretical treatment presented in Sections 7 and 8 it follows that in the presence of GVD and/or higher-order dispersion the amplitude of a grating required for pulse compression should be modulated to achieve a uniform conversion across the pulse spectrum. From a practical standpoint, it might be difficult to control the local duty cycle precisely enough to exactly reproduce the desired amplitude modulation, as given by Eq. (8.17) for the case of Gaussian pulses. We expect that, if a grating with no amplitude modulation is used, it would cause the shape of the SH spectrum to deviate from the assumed Gaussian form but should not introduce significant uncompensated phase on the SH pulse. Though intuitively reasonable, this assertion must be tested numerically. Another intuitive consideration is that, even though the necessary grating function for compression in the presence of GVD was derived in Section 8 under the assumption of Gaussian pulses, the distribution of the k-vector that is primarily responsible for phase compensation of the chirped FH pulse should also work for other pulse shapes, as long as the pulse spectrum is smooth. This insensitivity of the phase to the pulse shape has been noted before in the literature[31] and also appears from the stationary phase analysis results, Eqs. (7.11) and (7.8). The actual pulse shape enters the grating phase derivation procedure through the phase of $\hat{p}(z,\Omega)$, defined by the integral expression of Eq. (7.5); for smooth pulse shapes, $\angle\hat{p}(z,\Omega)$ is relatively insensitive to the actual pulse shape.

To address these issues as well as to test the results of Section 7 in the presence of dispersion terms higher than GVD, we simulate numerically the propagation of the coupled FH and SH waves based on the time-domain versions of Eqs. (4.3) and (4.4). We use the symmetrical split-step method[6,8]; the FFTW software library[32,33] is used to implement the fast-Fourier-transform routines.

To ascertain the quality of the generated SH pulses we use several measures. First, the pulses are characterized by their temporal FWHM of the intensity, as is conventional in the experimental literature. So far in this paper we have used the $1/e$ intensity temporal half-width, which is more convenient mathematically for Gaussian pulses. To distinguish the two pulse length measures we continue using notation τ for the temporal $1/e$ half-width and introduce notation $\Delta\tau$ for the temporal FWHM. For a Gaussian pulse, they are related to each other according to $\Delta\tau = 2\sqrt{\ln 2}\,\tau \approx 1.66\tau$.

The second pulse quality check that we perform is a comparison of the generated SH pulse with the ideal pulse, which would have been generated if the grating had not introduced spectral truncation and had exactly corrected the FH phase. We take the square of the input stretched FH pulse, calculate its Fourier transform, flatten the spectral phase, and use the inverse Fourier transform to obtain the ideal SH pulse profile, $B_2^{\mathrm{ideal}}(L,t)$:

$$B_2^{\mathrm{ideal}}(L,t) = \mathrm{IFT}|\mathrm{FT}\{[B_1(t)]^2\}|, \tag{9.1}$$

where FT and IFT denote the Fourier transform and the inverse Fourier transform, respectively.

The third parameter that we calculate for the generated SH pulse is the pulse length, $\Delta\tau^{\mathrm{TL}}$, of a transform-limited pulse, $B_2^{\mathrm{TL}}(L,t)$, which has the same spectral profile as the generated SH pulse, but with a flat spectral phase:

$$B_2^{\mathrm{TL}}(L,t) = \mathrm{IFT}|\mathrm{FT}[B_2(L,t)]|. \tag{9.2}$$

Comparison of $\Delta\tau^{\mathrm{TL}}$ and $\Delta\tau_2$ serves as a measure of how well the grating compensates the FH phase, independent of the amount of the spectral truncation that it introduces.

As a model, in these simulations we consider generation of a compressed SH pulse ($C_2 = 0$) by doubling a FH pulse from a Ti:sapphire oscillator at a wavelength of 800 nm with pulse length of $\Delta\tau_0 = 10\,\mathrm{fs}$ ($\tau_0 = 6\,\mathrm{fs}$), which is subsequently stretched to have chirp $C_1 = 10\tau_0^2$. The QPM grating is assumed to be fabricated on a lithium tantalate substrate, which has a lower nonlinearity than a more common ferroelectric for QPM, lithium niobate, but a deeper UV absorption edge, so that the two-photon absorption of the SH is of less concern. Also, it appears that the short QPM periods of $\sim 3.5\ \mu\mathrm{m}$ required for doubling of 800 nm are easier to pole in lithium tantalate.[34] The dispersion parameters are calculated from the Sellmeier data of Ref. 35 as $\Delta k_0 = -1.99\,\mu\mathrm{m}^{-1}$, $\delta\nu = -1.49\,\mathrm{ps/min}$, $\beta_1 = 305\,\mathrm{fs}^2/\mathrm{mm}$, and $\beta_2 = 1142\,\mathrm{fs}^2/\mathrm{mm}$, and the normalized GVD coefficients are $\beta_1/(\tau_0\delta\nu) = -34\times10^{-3}$ and $\beta_2/(\tau_0\delta\nu) = -127\times10^{-3}$. Note that, if one were to use a uniform QPM grating on the lithium tantalate substrate to double such short pulses, one would need to choose a grating length of $8\ \mu\mathrm{m}$ to avoid significant pulse broadening. Using such a short length poses problems of handling the crystal, and using confocal focusing to achieve high efficiency, requiring focusing into spot size of $0.7\ \mu\mathrm{m}$, is not practical. These issues do not emerge for longer crystals used with chirped pulses.

We numerically test the results of Section 8 for the case in which GVD at both the SH and the FH is nonnegligible. To separate the GVD effects from the higher-order dispersion effects we first set to zero the material's dispersion coefficients beyond GVD in the numerical propagation of the coupled fields. The effects of higher-order dispersion on the required grating function and the generated SH pulse are considered at the end of this section. The required grating length is obtained with Eq. (8.16) as $L = 0.213\,\mathrm{mm}$. Figure 6(a) (dashed curve) shows the grating period $\Lambda(z) = 2\pi/K(z)$, as obtained with Eq. (8.12). The required modulation of the grating amplitude $|d(z)|$ is obtained with Eq. (8.17) and is shown in Fig. 6(b) (dashed curve).

For the Gaussian linearly chirped FH pulse, $B_1(t)$ as defined by Eq. (6.4), the generated SH pulse profile, $B_2(L,t)$, is shown in Fig. 7 (dashed curve). The pulse length $\Delta\tau_2 = 7.7\,\mathrm{fs}$. This is 9% broader than the ideal SH pulse, $B_2^{\mathrm{ideal}}(L,t)$, as calculated with Eq. (9.1) and as shown in Fig. 7 (solid curve), which has a pulse width of $\Delta\tau_2 = \Delta\tau_0/\sqrt{2} = 7.1\,\mathrm{fs}$. This broadening results from the spectral truncation that is due to the finite grating length used. However, this spectral truncation does not introduce significant uncompensated phase, as can be

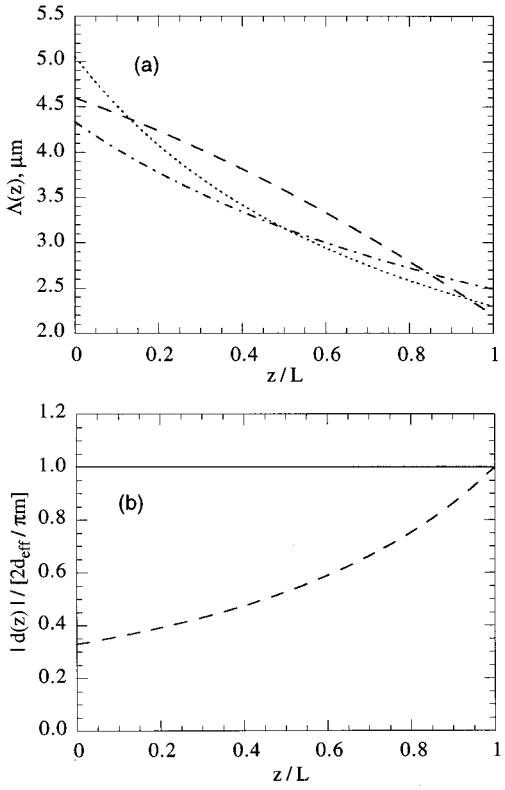

Fig. 6. (a) Distribution of the grating period $\Lambda(z)$ for compression in lithium tantalate. The dashed curve represents a grating designed according to the prescription of Section 8 to account for GVD at both the SH and the FH; the dotted–dashed curve, a linearly chirped grating designed according to Section 6 [Eqs. (6.6) and (6.12)] to account for GVD at the SH; the dotted curve, a linearly chirped grating designed without accounting for the GVD effects [Eqs. (6.6) and (6.9)]. (b) Distribution of the grating amplitude for a grating designed to account for GVD at both the SH and the FH [Eq. (8.11) (dashed curve)]. Also shown is the unmodulated amplitude of the grating (solid curve).

judged from Fig. 7(b); the calculation shows that $\Delta\tau_2$ is only 1.4% broader than $\Delta\tau^{\mathrm{TL}}$.

The required grating amplitude modulation is 67% [Fig. 6(b), dashed curve]. If instead a grating with a flat amplitude [Fig. 6(b), solid curve] is used, the resulting temporal profile of the compressed SH pulse is essentially indistinguishable in shape from the one obtained with the modulated grating amplitude, but the pulse has 2.7 times more energy. When the grating with unmodulated amplitude is used different spectral components convert with different efficiencies roughly linear with frequency, to first order, causing a slight shift of the whole SH pulse in time, but not changing the shape of the compressed pulse. If it is desirable to generate a chirped SH pulse, the nonuniformity of the conversion for different spectral components in a grating with unmodulated amplitude would have a more profound effect on the temporal shape of the SH pulse. Note that this insensitivity of the pulse quality to the amplitude modulation of the grating also means relatively high tolerance to QPM-grating fabrication errors. The positions of the inverted domains are determined by the lithography mask and hence can be considered error free. Poling defects affect only the local duty cycle of the grating and hence affect only the amplitude, but not the phase, of the Fourier component of the QPM grating.[10] Consequently, these errors do not lead to substantial pulse quality reduction. Of course, if several adjacent domains are completely missing, this could significantly affect the spectral content of the generated pulse.

It is instructive to see the extent to which the effects of GVD influence the generated SH pulse if the grating used is designed without accounting for GVD. In this case the grating is linearly chirped, its k-vector being given by Eq. (6.6), with the grating chirp calculated according to Eq. (6.9) as $D_g = 6.17 \times 10^3\,\mathrm{mm}^{-2}$, as shown in Fig. 6(a) (dotted curve). As can be seen, the grating function does not differ much from the grating with GVD correction; however, the SH pulse generated [as shown in Fig. 7 (dotted curve)] is almost two times broader, $\Delta\tau_2 = 13.7\,\mathrm{fs}$. The phase of the pulse has substantial curvature, resulting in $\Delta\tau_2$ being 1.79 times broader than $\Delta\tau^{\mathrm{TL}}$. If the grating chirp is selected according to Eq. (6.12) to compensate for the quadratic contribution to the phase, caused by the GVD at the SH [as shown in Fig. 6(a) (dotted–dashed curve)], the generated SH pulse [Fig. 7 (dotted–dashed curve)] is less broad, $\Delta\tau_2 = 10.4\,\mathrm{fs}$, but it still has ripples on the leading edge and substantial phase

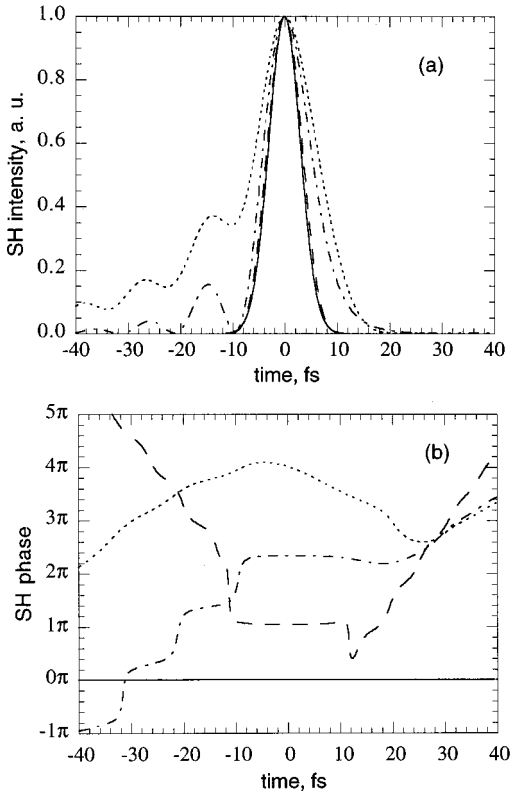

Fig. 7. (a) Intensities and (b) phases of the SH pulses obtained from a Gaussian FH pulse by use of different gratings. The dashed curve represents a grating designed to account for GVD at both the SH and the FH according to prescription of Section 8; the dotted–dashed curve, a grating designed to account for GVD at the SH [Eqs. (6.6) and (6.12)]; the dotted curve, a grating designed without accounting for the GVD effects [Eqs. (6.6) and (6.9)]. Also shown is the ideal SH pulse that would have been generated if the grating had not introduced spectral truncation and exactly corrected the FH phase (solid curve). Note that these results are obtained from the numerical simulations with dispersion terms beyond GVD set to zero.

variation across the pulse profile, resulting in $\Delta\tau_2$ being 1.20 times broader than $\Delta\tau^{TL}$.

Since we have seen for the Gaussian pulses that the grating amplitude modulation does not have a significant effect on the phase of the generated pulse, it also seems intuitively reasonable that the grating designed for linearly chirped Gaussian pulses should work well for other pulse shapes, as long as the phase of the stretched pulse is also predominantly quadratic. We test this assertion by propagating FH pulses with a hyperbolic secant temporal profile and with a super-Gaussian spectral profile through a grating with flat amplitude distribution and with the k-vector distribution as designed for a Gaussian FH pulse, according to Eq. (8.12) [Fig. 6(a) (solid curve)] and compare the results with pulses generated in gratings designed according to the prescription of Section 7 for the particular pulse shape.

For a hyperbolic secant FH pulse, the temporal profile before stretching is

$$B_1(t) = E_0 \operatorname{sech}(t/\tau_s), \tag{9.3}$$

where $\tau_s = \tau_0\sqrt{\ln 2}/\ln(1+\sqrt{2}) \approx 0.945\tau_0$ is selected such that its FWHM is equal to that of a Gaussian pulse with $1/e$ intensity half-width of τ_0. The SH pulse generated in a grating designed for a Gaussian pulse has length of $\Delta\tau_2 = 9.0$ fs, which is 6% broader than the ideal pulse profile, as a result of spectral truncation. The phase is essentially flat over the time range in which the pulse has substantial intensity, resulting in 1.4% broadening relative to the transform limit. Calculation of the grating k-vector according to the prescription of Section 7 for the hyperbolic secant pulse gives a result almost indistinguishable from that obtained for a Gaussian pulse; consequently, the SH pulses generated with these two gratings are of the same quality.

The input FH pulse with a super-Gaussian spectral profile is assumed to be of the form

$$\hat{B}_1(\Omega_1) = E_0 \exp\left[-\frac{(\tau_{sg}\Omega_1)^{2m}}{2}\right], \tag{9.4}$$

where we have chosen $m = 5$ and $\tau_{sg} = 0.621\tau_0$, with the numerical factor being selected such that the temporal intensity profile of the pulse whose spectrum is as given by Eq. (9.4) has the same FWHM as a Gaussian pulse whose $1/e$ intensity half-width is τ_0. The SH pulse generated in a grating designed for a Gaussian pulse has length of $\Delta\tau_2 = 6.0$ fs, 8% broader than the length of the ideal pulse. Comparison of $B_2(L,t)$ with $B_2^{TL}(L,t)$ shows that $\Delta\tau_2$ is only 1.1% broader than $\Delta\tau^{TL}$. As for the hyperbolic secant pulse, we also calculated the grating k-vector for the pulse with a super-Gaussian spectral profile, following the prescription of Section 7. The result is still very close to the k-vector designed for a Gaussian pulse; however, it shows a slightly larger difference, as compared with the hyperbolic secant. The SH pulse generated with the grating designed for this particular pulse shape was slightly shorter, $\Delta\tau_2 = 5.9$ fs, and slightly closer to the transform limit, being 0.7% broader than $\Delta\tau^{TL}$.

So far, the simulation results presented in this section have assumed negligible material dispersion beyond GVD. The utility of the approach developed in Section 7 can be seen especially well when this higher-order material dispersion is included in the pulse propagation simulations. We consider a Gaussian FH pulse and compare the SH pulses generated in the grating designed, according to Section 8, to account for the dispersion terms up to GVD and in the grating designed, according to Section 7, to account for the dispersion terms beyond GVD. In both cases the grating amplitude is assumed to be unmodulated. As can be seen from Fig. 8, dispersion beyond GVD has a noticeable effect. If this higher-order dispersion is not accounted for, the SH pulse [Fig. 8 (dotted–dashed curve)] has a pulse length of $\Delta\tau_2 = 8.8$ fs, which is 1.25 times broader than the length of the ideal pulse (solid curve), and the pulse is 15% broader than the transform limit. If the dispersion beyond GVD is accounted for in the design of the grating, the SH pulse [Fig. 8 (dashed curve)] has substantially better quality, and its pulse length of $\Delta\tau_2 = 7.7$ fs is 10% broader than ideal and is only 1.3% broader than the transform limit. The simulation results for a hyperbolic secant pulse and a pulse with super-Gaussian spectrum show similar behavior. We again find that the required grating k-vector is relatively insensitive to the particular pulse shape for which it is designed.

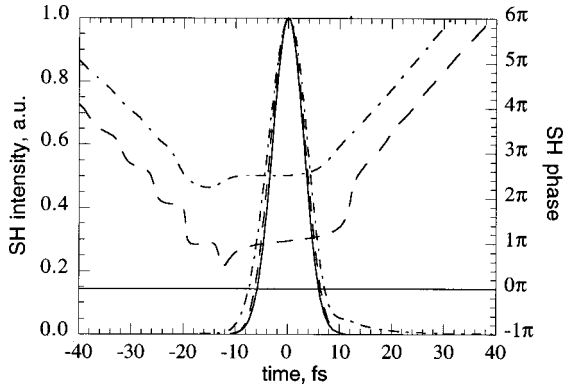

Fig. 8. SH pulses generated from a Gaussian FH pulse when the material dispersion beyond GVD is included in the simulations. The dashed curve represents the SH pulse obtained when the QPM grating is designed according to the prescription of Section 7 to completely account for the material dispersion; the dotted–dashed curve, the SH pulse generated in a grating designed to account for dispersion only up to the GVD terms (Section 8). In both cases grating amplitude is unmodulated. Also shown is the ideal SH pulse (solid curve).

As can be seen from this numerical modeling, the developed theory correctly predicts the grating k-vector distribution necessary to account for GVD and higher-order material dispersion. The SH pulse quality appears to be essentially independent of the pulse shape, at least for the three representative pulse shapes with smooth single-peaked spectra, in agreement with previous observations.[31] The generated SH pulses are consistently 7–10% broader than the ideal pulses, the effect caused by spectral truncation that is due to the finite grating length used. More importantly, the phase is compensated properly, giving pulses that are only ~1% broader than the transform limit. We also note that, regardless of whether the grating amplitude is modulated or kept flat, the quality of the generated compressed SH

pulse is not greatly affected; in contrast, the efficiency is several times better for gratings with no amplitude modulation. We note, however, that, if it is desirable to generate a chirped SH pulse, the grating amplitude modulation is necessary to avoid significant amplitude modulation of the SH pulse.

10. COMPARISON OF QUASI-PHASE-MATCHING FERROELECTRICS

In this section we provide, for reference, the dispersion data obtained from the published Sellmeier equations for several representative QPM ferroelectrics: lithium niobate,[36] lithium tantalate,[35] and KTP[37] (solid, dashed, and dotted curves, respectively, in Figs. 9–12). Figure 9 shows the QPM period as a function of the FH wavelength. Figure 10 shows the GVM coefficients $\delta\nu$ as functions of the FH wavelength. It is interesting that the $\delta\nu$ values for these materials are rather close to one another. Figure 11 shows both the GVD coefficient β_1 as a function of the FH wavelength and the SH GVD coefficient β_2 as a function of the FH wavelength that generates the corresponding SH.

The important parameters that enter the analytical treatment presented are the normalized GVD coefficients $\beta_i/\delta\nu\tau_0$; as pointed out in Section 8, the analysis is valid when $\beta_i/\delta\nu\tau_0 < 1$. Figure 12 shows $\beta_i/\delta\nu$ as functions

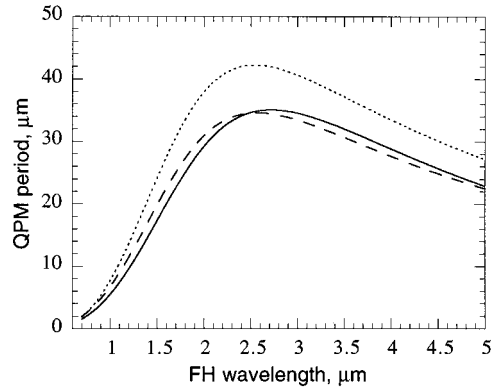

Fig. 9. QPM period as a function of FH wavelength in lithium niobate (solid curve), lithium tantalate (dashed curve), and KTP (dotted curve).

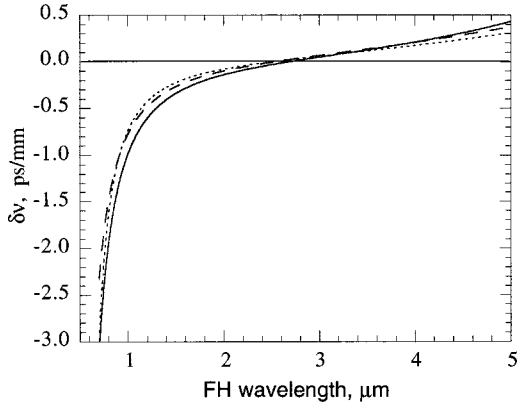

Fig. 10. GVM coefficient $\delta\nu$ as a function of FH wavelength in lithium niobate (solid curve), lithium tantalate (dashed curve), and KTP (dotted curve).

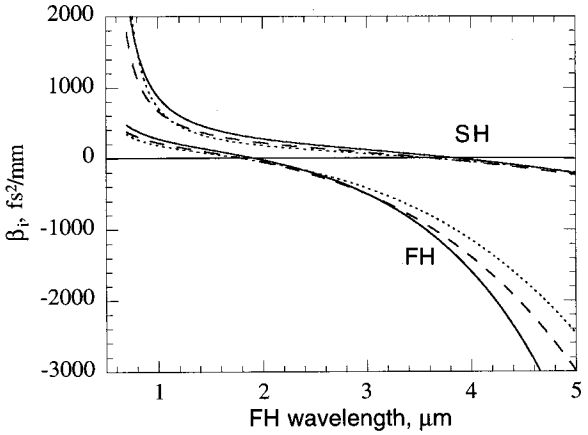

Fig. 11. FH GVD coefficient β_1 as a function of the FH wavelength, and the SH GVD coefficient β_2 as a function of the FH wavelength that generates the corresponding SH, in lithium niobate (solid curve), lithium tantalate (dashed curve) and KTP (dotted curve).

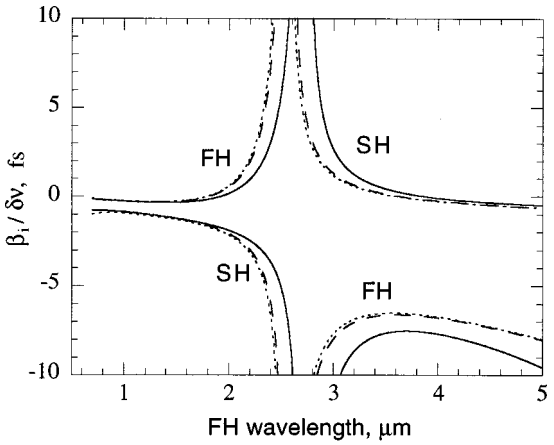

Fig. 12. Ratio $\beta_i/\delta\nu$ as a function of the FH wavelength in lithium niobate (solid curve), lithium tantalate (dashed curve), and KTP (dotted curve).

of the FH wavelength. We note that, except for the vicinity of the wavelengths at which $\delta\nu$ goes to zero (at around 2.7 μm), the condition $\beta_i/\delta\nu\tau_0 < 1$ is satisfied for pulses longer than $\approx$5 fs in the range $\lambda_1 < 2\ \mu$m and for pulses longer than $\approx$10 fs in the range $\lambda_1 > 3.2\ \mu$m.

11. SUMMARY

We have presented a theory of ultrafast SHG with longitudinally nonuniform gratings in the presence of GVD and higher-order dispersion. The developed approach gives an explicit prescription, valid for arbitrary material dispersion, for engineering the QPM grating necessary for a particular shaping function. The numerical simulations of propagation of the coupled FH and SH waves confirm the validity of the presented theory and predict that, when the dispersion is correctly accounted for, generation of sub-10-fs transform-limited pulses is possible by doubling of 10-fs pulses at a wavelength of 800 nm in a QPM grating fabricated on a lithium tantalate substrate.

Although the numerical simulations predict that generation of compressed sub-10-fs SH pulses at 400 nm of

good quality is possible, the theory does not account for other nonlinear effects that can spoil the pulse quality. In particular, the two-photon absorption (TPA) of the SH is of concern because the SH photon energy exceeds half the bandgap of lithium tantalate and because the peak intensity of ultrashort pulses is high. A possible way of alleviating the TPA is to reduce the SH peak intensity by generation of negatively chirped stretched pulses followed by external compression by simply passing the pulses through an appropriate length of a UV-transparent material. A theory that incorporates TPA in the description of the SHG process would be useful for the device performance optimization in the nonnegligible TPA regime, as would more-complete data for the spectral dependence of the TPA coefficients.

ACKNOWLEDGMENTS

This research was supported by Defense Advanced Research Projects Agency grant N00014-92-J-1903 through the Center for Nonlinear Optical Materials at Stanford University, by the Joint Services Electronics Program through Office of Naval Research grant N00014-91-J-1050, and by U.S. Air Force Office of Scientific Research grant F49620-99-1-0270. G. Imeshev and M. A. Arbore acknowledge support from IMRA America. We are grateful to Günter Steinmeyer for the help with numerical simulations and useful discussions. We appreciate many fruitful discussions with Almantas Galvanauskas and Donald Harter.

G. Imeshev can be reached by e-mail at gena@leland.stanford.edu.

*Present address, Lightwave Electronics, 2400 Charleston Road, Mountain View, California 94043.

†On leave from Ecole Polytechnique, 21128 Palaiseau Cedex, Paris, France.

REFERENCES

1. J. Comly and E. Garmire, "Second harmonic generation from short pulses," Appl. Phys. Lett. **12**, 7–9 (1968).
2. W. H. Glenn, "Second harmonic generation by picosecond optical pulses," IEEE J. Quantum Electron. **QE-5**, 284–290 (1969).
3. S. A. Akhmanov, A. P. Sukhorukov, and A. S. Chirkin, "Nonstationary phenomena and space–time analogy in nonlinear optics," Sov. Phys. JETP **28**, 748–757 (1969).
4. S. A. Akhmanov, V. A. Vysloukh, and A. S. Chirkin, *Optics of Femtosecond Laser Pulses* (American Institute of Physics, Melville, N.Y., 1992).
5. A. M. Weiner, "Effect of group velocity mismatch on the measurement of ultrashort optical pulses via second harmonic generation," IEEE J. Quantum Electron. **QE-19**, 1276–1283 (1983).
6. G. P. Agrawal, *Nonlinear Fiber Optics*, 2nd ed. (Academic, San Diego, Calif., 1995).
7. E. Sidick, A. Knoesen, and A. Dienes, "Ultrashort-pulse second harmonic generation. I. Transform-limited fundamental pulses," J. Opt. Soc. Am. B **12**, 1704–1712 (1995).
8. A. Knoesen, E. Sidick, and A. Dienes, in *Novel Optical Materials and Applications*, I.-C. Khoo, F. Simoni, and C. Umeton, eds. (Wiley, New York, 1997).
9. J. A. Armstrong, N. Bloembergen, and P. S. Pershan, "Interactions between light waves in a nonlinear dielectric," Phys. Rev. **127**, 1918–1939 (1962).
10. M. M. Fejer, G. A. Magel, D. H. Jundt, and R. L. Byer, "Quasi-phase-matched second harmonic generation: tuning and tolerances," IEEE J. Quantum Electron. **28**, 2631–2654 (1992).
11. M. A. Arbore, A. Galvanauskas, D. Harter, M. H. Chou, and M. M. Fejer, "Engineerable compression of ultrashort pulses by use of second-harmonic generation in chirped-period-poled lithium niobate," Opt. Lett. **22**, 1341–1343 (1997).
12. G. Imeshev, A. Galvanauskas, D. Harter, M. A. Arbore, M. Proctor, and M. M. Fejer, "Engineerable femtosecond pulse shaping by second-harmonic generation with Fourier synthetic quasi-phase-matching gratings," Opt. Lett. **23**, 864–866 (1998).
13. A. Galvanauskas, D. Harter, M. A. Arbore, M. H. Chou, and M. M. Fejer, "Chirped-pulse-amplification circuits for fiber amplifiers, based on chirped-period quasi-phase-matching gratings," Opt. Lett. **23**, 1695–1697 (1998).
14. A. Galvanauskas, A. Hariharan, D. Harter, M. A. Arbore, and M. M. Fejer, "Microlaser pumped, engineerable bandwidth parametric chirped-pulse amplifier using electric-field-poled $LiNbO_3$," in *Conference on Lasers and Electro-Optics*, Vol. 6 of 1998 Technical Digest Series (Optical Society of America, Washington, D.C., 1998), p. 16.
15. M. Hofer, M. E. Fermann, A. Galvanauskas, D. Harter, and R. S. Windeler, "Low-noise amplification of high-power pulses in multimode fibers," IEEE Photon. Technol. Lett. **11**, 650–652 (1999).
16. P. Loza-Alvarez, D. T. Reid, P. Faller, M. Ebrahimzadeh, W. Sibbett, H. Karlsson, and F. Laurell, "Simultaneous femtosecond-pulse compression and second-harmonic generation in aperiodically poled $KTiOPO_4$," Opt. Lett. **24**, 1071–1073 (1999).
17. P. Loza-Alvarez, D. T. Reid, P. Faller, M. Ebrahimzadeh, and W. Sibbett, "Simultaneous second-harmonic generation and femtosecond-pulse compression in aperiodically poled $KTiOPO_4$ with a $RbTiOAsO_4$-based optical parametric oscillator," J. Opt. Soc. Am. B **16**, 1553–1560 (1999).
18. M. A. Arbore, O. Marco, and M. M. Fejer, "Pulse compression during second-harmonic generation in aperiodic quasi-phase-matching gratings," Opt. Lett. **22**, 865–867 (1997).
19. G. Imeshev, M. A. Arbore, M. M. Fejer, A. Galvanauskas, M. Fermann, and D. Harter, "Ultrashort-pulse second-harmonic generation with longitudinally nonuniform quasi-phase-matching gratings: pulse compression and shaping," J. Opt. Soc. Am. B **17**, 304–318 (2000).
20. M. L. Sundheimer, A. Villeneuve, G. I. Stegeman, and J. D. Bierlein, "Simultaneous generation of red, green and blue light in a segmented KTP waveguide using a single source," Electron. Lett. **30**, 975–976 (1994).
21. P. Baldi, C. G. Trevino-Palacios, G. I. Stegeman, M. P. De Micheli, D. B. Ostrowsky, D. Delacourt, and M. Papuchon, "Simultaneous generation of red, green and blue light in room temperature periodically poled lithium niobate waveguides using single source," Electron. Lett. **31**, 1350–1351 (1995).
22. O. Pfister, J. S. Wells, L. Hollberg, L. Zink, D. A. Van Baak, M. D. Levenson, and W. R. Bosenberg, "Continuous-wave frequency tripling and quadrupling by simultaneous three-wave mixings in periodically poled crystals: application to a two-step 1.19–10.71-μm frequency bridge," Opt. Lett. **22**, 1211–1213 (1997).
23. G. Imeshev, M. A. Arbore, A. Galvanauskas, and M. M. Fejer, "Numerical simulations of ultrafast SHG with chirped QPM gratings in the pump-depleted regime," Center for Nonlinear Optical Materials annual report (Stanford University, Stanford, Calif., 1997).
24. V. G. Dmitriev and S. G. Grechin, "Multi frequency laser radiation harmonics generation in nonlinear crystals with regular domain structure," in *ICONO '98: Nonlinear Optical Phenomena and Coherent Optics in Information Technologies*, S. S. Chesnokov, V. P. Kandidov, and N. I. Koroteev, eds., Proc. SPIE **3733**, 228–236 (1999).

25. S. Saltiel and Y. Deyanova, "Polarization switching as a result of cascading of two simultaneously phase-matched quadratic processes," Opt. Lett. **24**, 1296–1298 (1999).
26. M. S. Webb, D. Eimerl, and S. P. Velsko, "Wavelength insensitive phase-matched second-harmonic generation in partially deuterated KDP," J. Opt. Soc. Am. B **9**, 1118–1127 (1992).
27. S. Lin, B. Wu, F. Xie, and C. Chen, "Phase matching retracing behavior for second harmonic generation in LiB_3O_5 crystal," J. Appl. Phys. **73**, 1029–1034 (1993).
28. S. K. Kurtz, in *Quantum Electronics: A Treatise*, H. Rabin and C. L. Tang, eds. (Academic, New York, 1975).
29. C. M. Bender and S. A. Orszag, *Advanced Mathematical Methods for Scientists and Engineers* (McGraw-Hill, New York, 1978).
30. D. Zwillinger, *Handbook of Integration* (Jones and Bartlett, Sudbury, Mass., 1992).
31. E. Sidick, A. Knoesen, and A. Dienes, "Ultrashort-pulse second harmonic generation. II. Non-transform-limited fundamental pulses," J. Opt. Soc. Am. B **12**, 1713–1722 (1995).
32. M. Frigo and S. G. Johnson, "FFTW: an adaptive software architecture for the FFT," IEEE Trans. Acoust. Speech Signal Process. **3**, 1381–1384 (1998).
33. The FFTW software is available for downloading at http://www.fftw.org.
34. J.-P. Meyn, Universität Kaiserslautern, D-67663 Kaiserslautern, Germany (personal communication, 1999).
35. J.-P. Meyn and M. M. Fejer, "Tunable ultraviolet radiation by second-harmonic generation in periodically poled lithium tantalate," Opt. Lett. **22**, 1214–1216 (1997).
36. D. H. Jundt, "Temperature-dependent Sellmeier equation for the index of refraction, n_e, in congruent lithium niobate," Opt. Lett. **22**, 1553–1555 (1997).
37. L. K. Cheng, L. T. Cheng, J. Galperin, P. A. Morris Hotsenpiller, and J. D. Bierlein, "Crystal growth and characterization of $KiTiOPO_4$ isomorphs from the self-fluxes," J. Cryst. Growth **137**, 107–115 (1994).